

Radiation processes in dielectric cylindrical waveguides

A. A. Saharian^{1,2*}, L. Sh. Grigoryan², H. F. Khachatryan²

¹*Institute of Physics, Yerevan State University,
1 Alex Manoogian Street, 0025 Yerevan, Armenia*

²*Institute of Applied Problems of Physics NAS RA,
25 Hrachya Nersissyan Street, 0014 Yerevan, Armenia*

January 8, 2026

Abstract

Dielectric cylindrical waveguides are widely used for confining and guiding of electromagnetic waves in relatively wide range of frequencies. They have found numerous technological and scientific applications in telecommunications, medicine, material science, photonics and quantum optics. The electromagnetic field Green function is the central object in investigations of different types of radiation processes in those structures. In this paper, we review and further develop the recurrence procedure for evaluating the electromagnetic field Green function in a medium made of any number of homogeneous cylindrical layers. The general results are specified for a cylindrical waveguide immersed in a homogeneous medium. Expressions are provided for all the components of the Green tensor in both regions inside and outside the cylinder. As an application of the results for the Green function, we consider the radiation of a charged particle rotating around a dielectric cylinder. The intensities for all types of radiation processes are discussed. They include the synchrotron-Cherenkov radiation at large distances from the cylinder and the radiation on guided and surface polaritonic modes confined inside or near the surface of the cylinder. The paper provides explicit formulas for the electromagnetic fields and the spectral-angular densities of those radiations. It also includes a numerical and comparative analysis.

Key words: Dielectric waveguide; Green function; Synchrotron-Cherenkov radiation; Surface polaritons

1 Introduction

The interaction of charged particles with a medium can result in various radiation processes. One important type of this phenomenon is polarization radiation, which occurs when the medium is polarized by the particle's electromagnetic field. In these processes, charged particles act as indirect sources of radiation; the direct source is the medium's polarization relaxation. Polarization radiation is exemplified by well-known phenomena such as Cherenkov radiation [1]-[3], transition radiation [4]-[7], and diffraction radiation [8, 9]. Interest in these radiation processes stems from their ability to act as controllable sources of radiation across a broad spectrum of frequencies. These processes are also widely used to investigate the electromagnetic characteristics of media, for particle beam diagnostics, and in particle detectors.

*E-mail: saharian@ysu.am

Tuning the parameters of radiation sources, the electrodynamic characteristics of the media, and the geometry of their interfaces can effectively control the characteristics of generated radiation and its subsequent propagation. Recent technological advances in designing metamaterials, photonic crystals, and nanoscale structures offer new opportunities for manipulating the electric and magnetic characteristics of materials. In particular, the possibility for the control of dispersion relations for dielectric permittivity and permeability is of great importance [10, 11]. Significant progress in metamaterial-related research has led to the stimulation of active theoretical and experimental investigations of radiation processes in those media. Of particular interest is the interaction of charged particles with media whose permittivity and permeability become negative in certain spectral ranges.

Cylindrical waveguides are essential components used to guide electromagnetic waves at microwave, millimeter wave, and optical frequencies in modern communication systems and integrated photonic devices, including optical amplifiers, modulators, and lasers [12, 13]. They also play an important role in various fields of fundamental physics, including light-matter interactions, radiation mechanisms, dispersion relations of materials, boundary effects, particle beam manipulation and diagnostics, and dielectric wakefield acceleration. The wide range of applications of cylindrical waveguides motivates the investigation of different types of radiation processes in these structures. A great deal of research has been dedicated to the topic of energy losses of charged particles when they interact with cylindrical guiding structures (see, e.g., [14]-[61] and references therein). In these papers, different types of cylindrically symmetric dielectric structures inside a waveguide are discussed as well. Depending on the geometry of these structures, the generated radiation is a superposition of Cherenkov, transition, and diffraction radiations. In the main part of the cited references the charged particles move along rectilinear trajectories parallel to the axis of the waveguide. More complicated problems with charges rotating inside or outside a cylindrical waveguide were considered in references [23, 25, 27, 29, 31, 38, 48, 51, 53]. The features of the radiation in the case of helical motion are discussed in [41, 42, 44]. In these problems the radiation field is a superposition of Cherenkov and synchrotron radiations. Already for a charge rotating in a homogeneous medium, this superposition gives interesting interference features [2],[62]-[67]. The analysis of radiation processes in more complicated cylindrically symmetric geometries of waveguides, including those with conical elements, and the corresponding approximate analytic and numerical methods for study of radiation features can be found in [45],[68]-[76].

The present article aims to accomplish several objectives. In the first part, we review and further develop the recurrence procedure described in [23] for evaluating the electromagnetic field Green function in a medium consisting of general number of homogeneous cylindrical layers. Here, we provide explicit expressions for the coefficients of the radial parts of the Green function components in separate layers. The general results are specified for a cylindrical waveguide immersed in a homogeneous medium. In this case, the expressions are given for all the components of the Green tensor in both regions inside and outside the cylinder. This procedure has been used in a number of papers for the investigation of radiation from charged particles interacting with a dielectric cylinder. In the previously discussed problems, depending on the law of particle motion, the separate components required in those problems were considered. Knowledge of all the components makes it possible to study radiation processes in the case of a general law of particle motion. In the second part of the paper, as an application of the results for the Green function, we consider the radiation of a charged particle rotating around a dielectric cylinder. The intensities for all types of radiation processes are discussed. They include the synchrotron-Cherenkov radiation at large distances from the cylinder, the radiations on guided and surface polaritonic modes of the cylinder. Explicit formulas for the electromagnetic fields and the spectral-angular densities of those radiations are provided. This part of the paper combines some results from our previous studies.

The organization of the paper is as follows. In the next section, we describe the electromagnetic field Green function and its relations to the field potentials in an inhomogeneous medium with cylindrically symmetric dielectric function. In Section 3, a recurrence scheme is developed for the evaluation of the Green function in the special case of medium consisting general number of homogeneous cylindrical

layers. The construction of the so-called "potential-free" Green function, required at the initial stage of the recurrent procedure, is presented in Section 4. In Section 5, the general scheme is specified for a homogeneous dielectric cylindrical waveguide immersed in a homogeneous medium. All the components of the Green function are presented inside and outside the waveguide. The general features of the radiation processes in that setup are discussed in Section 6. Different types of the radiation modes and their dispersion relations are considered and the possibility for the appearance of strong narrow peaks in the angular distribution of the radiation propagating in the exterior medium is emphasized. As an radiation source, Section 7 considers a point charge coaxially circulating around a dielectric cylinder. The expressions for the Fourier components of the scalar and vector potentials, and for the electric and magnetic fields are presented in both interior and exterior regions. The radiation propagating in the exterior medium, at large distances from the cylinder, is discussed in Section 8. It presents the interference of the synchrotron and Cherenkov radiations influenced by the dielectric cylinder. A formula is derived for the spectral-angular density of the radiation intensity and the presence of strong narrow peaks in the angular distribution of the radiation on a given harmonic is demonstrated. In Section 9, we consider the radiation on normal modes of a cylindrical waveguide. The corresponding contributions to the electric and magnetic fields originate from the poles of the Green function. Explicit expressions for those parts in the fields and for energy fluxes through a plane, perpendicular to the cylinder axis, are provided. The energy fluxes and the radiated power for surface polaritons are studied in Section 10. The features of the distribution of the radiated normal modes are discussed and numerical examples are presented. Section 11 summarizes the main results of the paper.

2 Electromagnetic Green function in cylindrically symmetric media

The Green function (GF) plays a central role in the study of classical and quantum electrodynamic effects in media. We consider the electromagnetic field generated by the current density $\mathbf{j}(x)$ and charge density $\rho(x)$ in a cylindrically symmetric, nonmagnetic medium with dielectric permittivity $\hat{\varepsilon}$. Here and below, $x = (t, \mathbf{r})$ stands for spacetime coordinates. In the Lorentz gauge

$$\nabla \cdot \mathbf{A} + \frac{\hat{\varepsilon}}{c} \partial_t \varphi = 0, \quad (2.1)$$

for the scalar and vector potentials $\varphi(x)$ and $\mathbf{A}(x)$, the Maxwell's equations read

$$\left(\Delta - \frac{\hat{\varepsilon}}{c^2} \partial_t^2 \right) \mathbf{A} - \hat{\varepsilon}^{-1} (\nabla \hat{\varepsilon}) \nabla \cdot \mathbf{A} = -\frac{4\pi}{c} \mathbf{j}, \quad (2.2)$$

$$\left(\Delta - \frac{\hat{\varepsilon}}{c^2} \partial_t^2 \right) \varphi + \hat{\varepsilon}^{-1} (\nabla \hat{\varepsilon}) \cdot \left(\nabla \varphi + \frac{1}{c} \partial_t \mathbf{A} \right) = -4\pi \hat{\varepsilon}^{-1} \rho. \quad (2.3)$$

The charge and current densities are related by the continuity equation $\partial_t \rho + \nabla \cdot \mathbf{j} = 0$. Introducing the cylindrical coordinate system (r, ϕ, z) , the equation (2.2) for the vector potential in a cylindrically symmetric medium with $\hat{\varepsilon} = \hat{\varepsilon}(r)$ is presented in the form

$$\left[\hat{\mathcal{F}}_{il} - \hat{\varepsilon}^{-1} (\partial_r \hat{\varepsilon}) \hat{\mathcal{D}}_{il} \right] A_l = -\frac{4\pi}{c} j_i, \quad (2.4)$$

where the indices $i, l = 1, 2, 3$ correspond to the components along the coordinates r, ϕ, z and a summation is understood over repeated indices. In (2.4), the matrix operators $\hat{\mathcal{F}}$ and $\hat{\mathcal{D}}$ with the matrix elements \mathcal{F}_{il} and \mathcal{D}_{il} are given by the expressions

$$\hat{\mathcal{F}} = \begin{pmatrix} \Delta - r^{-2} - \frac{\hat{\varepsilon}}{c^2} \partial_t^2 & -2r^{-2} \partial_\phi & 0 \\ 2r^{-2} \partial_\phi & \Delta - r^{-2} - \frac{\hat{\varepsilon}}{c^2} \partial_t^2 & 0 \\ 0 & 0 & \Delta - \frac{\hat{\varepsilon}}{c^2} \partial_t^2 \end{pmatrix}, \quad (2.5)$$

and

$$\hat{\mathcal{D}} = \begin{pmatrix} 1/r + \partial_r & r^{-1}\partial_\phi & \partial_z \\ 0 & 0 & 0 \\ 0 & 0 & 0 \end{pmatrix}, \quad (2.6)$$

where Δ is the Laplace operator in cylindrical coordinates.

We introduce the electromagnetic field retarded GF $G_{il}(x, x')$ related to the operator in the right-hand side of (2.4). Introducing the 3×3 matrix $\hat{G}(x, x')$, with the elements $G_{il}(x, x')$, the equation for the GF reads

$$[\hat{\mathcal{F}} - \hat{\varepsilon}^{-1}(\partial_r \hat{\varepsilon}) \hat{\mathcal{D}}] G(x, x') = (2\pi)^3 I \delta(x - x'), \quad (2.7)$$

where I is the 3×3 unit matrix. Given the GF, the solution of the equation (2.4) is presented in the form

$$A_i(x) = -\frac{1}{2\pi^2 c} \int d^4 x' G_{il}(x, x') j_l(x'). \quad (2.8)$$

For static and cylindrically symmetric medium we use the partial Fourier transform

$$\hat{G}(x, x') = \sum_{n=-\infty}^{+\infty} \int_{-\infty}^{+\infty} dk \int_{-\infty}^{+\infty} d\omega \hat{G}_n(k, \omega, r, r') e^{in(\phi-\phi')+ik(z-z')-i\omega(t-t')}, \quad (2.9)$$

where $x = (t, r, \phi, z)$ and $x' = (t', r', \phi', z')$. The matrix elements of the Fourier image $\hat{G}_n(k, \omega, r, r')$ will be denoted by $G_{il,n}(k, \omega, r, r')$. From (2.7) we get the equation for the Fourier image $\hat{G}_n(k, \omega, r, r') \equiv \hat{G}_n(r, r')$:

$$\left[\hat{F} - \frac{\partial_r \varepsilon(r)}{\varepsilon(r)} \hat{\mathcal{D}} \right] \hat{G}_n(r, r') = \frac{I}{r'} \delta(r - r'), \quad (2.10)$$

with the dielectric permittivity $\varepsilon(r) = \varepsilon(\omega, r)$. The matrix operators \hat{F} and $\hat{\mathcal{D}}$ are defined by

$$\hat{F}(r) = \begin{pmatrix} \hat{f}(r) & -2in/r^2 & 0 \\ 2in/r^2 & \hat{f}(r) & 0 \\ 0 & 0 & \hat{f}(r) + 1/r^2 \end{pmatrix}, \quad (2.11)$$

$$\hat{\mathcal{D}}(r) = \begin{pmatrix} 1/r + \partial_r & in/r & ik \\ 0 & 0 & 0 \\ 0 & 0 & 0 \end{pmatrix}, \quad (2.12)$$

where

$$\hat{f}(r) = \frac{1}{r} \partial_r(r \partial_r) - \frac{n^2 + 1}{r^2} + \lambda^2, \quad (2.13)$$

and

$$\lambda = \frac{\omega}{c} \sqrt{\varepsilon(r) - c^2 k^2 / \omega^2}. \quad (2.14)$$

Expansions similar to (2.9) can also be written for the electromagnetic potentials:

$$\begin{Bmatrix} A_i(x) \\ \varphi(x) \end{Bmatrix} = \sum_{n=-\infty}^{+\infty} \int_{-\infty}^{+\infty} dk \int_{-\infty}^{+\infty} d\omega \begin{Bmatrix} A_{i,n}(k, \omega, r) \\ \varphi_n(k, \omega, r) \end{Bmatrix} e^{in\phi + ikz - i\omega t}. \quad (2.15)$$

The relation between the Fourier components of the vector potential and the current density is obtained from (2.9):

$$A_{i,n}(k, \omega, r) = -\frac{4\pi}{c} \int_0^\infty dr' r' G_{il,n}(k, \omega, r, r') j_{l,n}(k, \omega, r'), \quad (2.16)$$

where

$$j_{l,n}(k, \omega, r) = \frac{1}{(2\pi)^3} \int_0^{2\pi} d\phi \int_{-\infty}^{+\infty} dz \int_{-\infty}^{+\infty} dt j_l(x) e^{-in\phi - ikz + i\omega t}, \quad (2.17)$$

is the Fourier image of the current density. Having the vector potential, the Fourier component of the scalar potential is found from the Lorentz gauge condition (2.1):

$$\varphi_n(k, \omega, r) = \frac{c}{\omega \varepsilon(r)} \left[\frac{n}{r} A_{2,n}(k, \omega, r) + k A_{3,n}(k, \omega, r) - \frac{i}{r} \partial_r (r A_{1,n}(k, \omega, r)) \right]. \quad (2.18)$$

The strengths of the electric and magnetic fields are determined using the standard relations with the potentials.

3 Recurrence scheme for evaluation of the GF in cylindrically stratified media

In this section, we will consider a special case of the general setup presented in the previous section. The medium consists of N homogeneous cylindrical layers with dielectric permittivities $\varepsilon_0, \varepsilon_1, \dots, \varepsilon_N$. The radial dependence of the dielectric function is given by

$$\varepsilon(r) = \varepsilon(\omega, r) = \varepsilon_0 + \sum_{s=1}^N (\varepsilon_s - \varepsilon_{s-1}) \theta(r - r_s), \quad (3.1)$$

where $\theta(y)$ is the Heaviside unit step function and $\varepsilon_s = \varepsilon_s(\omega)$ for $s = 0, 1, \dots, N$. Substituting this in (2.10), we get the equation for the Fourier image of the GF:

$$\left[\hat{F}(r) - \sum_{s=1}^N \hat{A}^{(s)}(r) \right] \hat{G}_n(r, r') = \frac{I}{r'} \delta(r - r'), \quad (3.2)$$

where the matrix \hat{F} is given by (2.11) with dielectric permittivity (3.1) in the definition (2.14) of λ , and

$$\hat{A}^{(s)}(r) = \frac{\varepsilon_s - \varepsilon_{s-1}}{\varepsilon(r)} \delta(r - r_s) \hat{D}(r). \quad (3.3)$$

The terms in (3.2) with the functions $\hat{A}^{(s)}(r)$ can be interpreted as delta-type "interaction potentials" localized on the separating boundaries between homogeneous media.

We define the 3×3 Green function $\hat{G}_n^{(0)}(r, r')$, with the elements $G_{il,n}^{(0)}(r, r')$, by the equation

$$\hat{F}(r) \hat{G}_n^{(0)}(r, r') = \frac{I}{r'} \delta(r - r'). \quad (3.4)$$

For $\varepsilon(r) = \text{const}$ it reduces to the GF for a homogeneous medium. The equation (3.4) is obtained from (3.2) in the limit of zero delta-type "potentials" (3.3). In this sense, the function $\hat{G}_n^{(0)}(r, r')$ can be called a "potential-free" GF. With this function, the equation (3.2) can be rewritten in the form of Lipmann-Schwinger equation

$$\hat{G}_n(r, r') = \hat{G}_n^{(0)}(r, r') + \sum_{s=1}^N \int_0^\infty dr'' r'' \hat{G}_n^{(0)}(r, r'') \hat{A}^{(s)}(r'') \hat{G}_n(r'', r'). \quad (3.5)$$

Let us introduce intermediate 3×3 matrices $\hat{G}_n^{(s)}(r, r')$, $s = 1, 2, \dots, N$, defined by the relations

$$\hat{G}_n^{(s)}(r, r') = \hat{G}_n^{(s-1)}(r, r') + \int_0^\infty dr'' r'' \hat{G}_n^{(s-1)}(r, r'') \hat{A}^{(s)}(r'') \hat{G}_n^{(s)}(r'', r'). \quad (3.6)$$

Writing this equation for s replaced by $s - 1$ and putting the corresponding expression for $\hat{G}_n^{(s-1)}(r, r')$ in (3.6), it is seen that

$$\hat{G}_n^{(s)}(r, r') = \hat{G}_n^{(s-2)}(r, r') + \int_0^\infty dr'' r'' \hat{G}_n^{(s-2)}(r, r'') \left[\hat{A}^{(s-1)}(r'') + \hat{A}^{(s)}(r'') \right] \hat{G}_n^{(s)}(r'', r'). \quad (3.7)$$

Repeating this procedure, we get

$$\hat{G}_n^{(s)}(r, r') = \hat{G}_n^{(s-i)}(r, r') + \int_0^\infty dr'' r'' \hat{G}_n^{(s-i)}(r, r'') \sum_{l=s+1-i}^s \hat{A}^{(l)}(r'') \hat{G}_n^{(s)}(r'', r'). \quad (3.8)$$

For $s = i = N$, this equation is reduced to (3.5) and, hence, $\hat{G}_n^{(N)}(r, r') = \hat{G}_n(r, r')$.

By taking into account the expression (3.3) for $\hat{A}^{(s)}(r)$ in (3.6), one finds

$$G_n^{(s)}(r, r') = G_n^{(s-1)}(r, r') + (\varepsilon_s - \varepsilon_{s-1}) r_s G_n^{(s-1)}(r, r_s) \frac{\hat{D}(r'')}{\varepsilon(r'')} G_n^{(s)}(r'', r')|_{r''=r_s}. \quad (3.9)$$

Here and below, for a given function $g(r, r')$, the substitution $r = r_s$ is understood in the sense

$$\frac{\hat{D}(r)}{\varepsilon(r)} g(r, r')|_{r=r_s} = \frac{\hat{D}(r)}{2\varepsilon_{s-1}} g(r, r')|_{r=r_s-0} + \frac{\hat{D}(r)}{2\varepsilon_s} g(r, r')|_{r=r_s+0}. \quad (3.10)$$

Acting on (3.9) from the left by $(1/\varepsilon(r))\hat{D}(r)$ and then taking $r = r_s$, we obtain

$$\left[I - \hat{S}_s(r_s, r_s) \right] (\varepsilon_s - \varepsilon_{s-1}) r_s \frac{\hat{D}(r)}{\varepsilon(r)} \hat{G}_n^{(s)}(r, r')|_{r=r_s} = \hat{S}_s(r_s, r'), \quad (3.11)$$

where we have introduced the 3×3 matrix

$$\hat{S}_s(r_s, r') = (\varepsilon_s - \varepsilon_{s-1}) r_s \frac{\hat{D}(r)}{\varepsilon(r)} \hat{G}_n^{(s-1)}(r, r')|_{r=r_s}, \quad (3.12)$$

in the sense of (3.10).

The relation (3.11) allows us to find the quantity (3.10) appearing in the right-hand side of (3.9). To do so, note that, according to the definition (2.12) of the matrix operator $\hat{D}(r)$, for the elements of the matrix $\hat{S}_s(r_s, r')$ one has $S_{s,il}(r_s, r') = 0$ for $i = 2, 3$. For this type of matrices, the relation

$$\left[I - \hat{S}_s(r_s, r') \right]^{-1} = I + \frac{\hat{S}_s(r_s, r')}{1 - \text{Sp } \hat{S}_s(r_s, r')}, \quad (3.13)$$

holds. By taking into account this relation, from (3.11) we obtain

$$(\varepsilon_s - \varepsilon_{s-1}) r_s \frac{\hat{D}(r)}{\varepsilon(r)} \hat{G}_n^{(s)}(r, r')|_{r=r_s} = \left[I + \frac{\hat{S}_s(r_s, r_s)}{1 - \text{Sp } \hat{S}_s(r_s, r_s)} \right] \hat{S}_s(r_s, r'). \quad (3.14)$$

Substituting this in the relation (3.9) one finds

$$\hat{G}_n^{(s)}(r, r') = \hat{G}_n^{(s-1)}(r, r') + \hat{G}_n^{(s-1)}(r, r_s) \left[I + \frac{\hat{S}_s(r_s, r_s)}{1 - \text{Sp } \hat{S}_s(r_s, r_s)} \right] \hat{S}_s(r_s, r'). \quad (3.15)$$

This provides the recurrence relation which allows to find the GF $\hat{G}_n^{(s)}(r, r')$ having the function $\hat{G}_n^{(s-1)}(r, r')$. Note that for the elements $S_{s,il}(r_s, r')$ of the matrix $\hat{S}_s(r_s, r')$ we have $S_{s,il}(r_s, r') = 0$ for $i = 2, 3$ and, hence, $\text{Sp } \hat{S}_s(r_s, r_s) = S_{s,11}(r_s, r')$. By taking into account that $S_{s,il}(r_s, r') = 0$ for $i = 2, 3$, the relation

$$\left[I + \frac{\hat{S}_s(r_s, r_s)}{1 - \text{Sp } \hat{S}_s(r_s, r_s)} \right] \hat{S}_s(r_s, r') = \frac{\hat{S}_s(r_s, r')}{1 - \text{Sp } \hat{S}_s(r_s, r_s)}, \quad (3.16)$$

can be proved. With this result, the formula (3.15) is rewritten in a simpler form (an alternative representation is given in [23])

$$\hat{G}_n^{(s)}(r, r') = \hat{G}_n^{(s-1)}(r, r') + \frac{\hat{G}_n^{(s-1)}(r, r_s) \hat{S}_s(r_s, r')}{1 - \text{Sp } \hat{S}_s(r_s, r_s)}, \quad (3.17)$$

for $s = 1, 2, \dots, N$ and $\hat{G}_n(r, r') = \hat{G}_n^{(N)}(r, r')$. The formula (3.17) provides a recurrence relation for finding the GF $\hat{G}_n(r, r')$ given the function $\hat{G}_n^{(0)}(r, r')$.

4 Construction of the function $\hat{G}^{(0)}(r, r')$

In accordance with the results obtained in the previous section, the starting point of the determination of the GF is the evaluation of the function $\hat{G}_n^{(0)}(r, r')$, which obeys the equation (3.4). To diagonalize this matrix equation, we perform the transformation

$$\hat{G}_n^{(0)'}(r, r') = \hat{M}^{-1} \hat{G}_n^{(0)}(r, r') \hat{M}, \quad \hat{F}'(r) = \hat{M}^{-1} \hat{F}(r) \hat{M}, \quad (4.1)$$

with the matrix

$$\hat{M} = \begin{pmatrix} 1 & -i\delta_n & 0 \\ -i\delta_n & 1 & 0 \\ 0 & 0 & 1 \end{pmatrix}, \quad \delta_n = 1 - \delta_{n0}. \quad (4.2)$$

In the new representation, the equation (3.4) takes the form

$$\hat{F}'(r) \hat{G}_n^{(0)'}(r, r') = \frac{I}{r} \delta(r - r'), \quad (4.3)$$

with the diagonal matrix operator

$$\hat{F}'(r) = \text{diag} \left(\hat{f}(r) - \frac{2n}{r^2}, \hat{f}(r) + \frac{2n}{r^2}, \hat{f}(r) + \frac{1}{r^2} \right), \quad (4.4)$$

and with $\hat{f}(r)$ given by (2.13).

The solution of the equation (4.3) is presented as

$$\hat{G}_n^{(0)'}(r, r') = \text{diag} (g_{n+1}, g_{n-1}, g_n), \quad (4.5)$$

where the function $g_n = g_n(r, r')$ obeys the equation

$$\left[\hat{f}(r) + \frac{1}{r^2} \right] g_n(r, r') = \frac{1}{r} \delta(r - r'). \quad (4.6)$$

The solution for $\hat{G}^{(0)}(r, r')$ is obtained by inverting the transformation (4.1). For $n \neq 0$ we get

$$\hat{G}_n^{(0)}(r, r') = \frac{1}{2} \begin{pmatrix} g_{n+1} + g_{n-1} & i(g_{n+1} - g_{n-1}) & 0 \\ -i(g_{n+1} - g_{n-1}) & g_{n+1} + g_{n-1} & 0 \\ 0 & 0 & 2g_n \end{pmatrix}, \quad (4.7)$$

and for $n = 0$ one obtains $\hat{G}_0^{(0)}(r, r') = \text{diag}(g_1, g_1, g_0)$. Note that the latter is obtained from (4.7) taking $n = 0$ and $g_{-1} = g_1$. The functions $g_{\pm 1}(r, r')$ are the solutions of the same equation (4.6).

The result (4.7) is valid for general case of cylindrically symmetric dielectric permittivity $\varepsilon(r) = \varepsilon(\omega, r)$, with λ in (2.13) defined by (2.14). For a stratified medium with homogeneous cylindrical layers, the permittivity is given by (3.1) with constant dielectric functions $\varepsilon_i = \varepsilon_i(\omega)$, $i = 0, 1, 2, \dots, N$. In this case the equation (4.6) for the function $g_n(r, r')$ in separate layers is reduced to the Bessel equation for $r \neq r'$. Let $r_j < r' < r_{j+1}$. Then, in the layer $r_i < r < r_{i+1}$ with $i \neq j$, the solution to the equation (4.6) is a linear combination of the Bessel function $J_n(y)$ and the Hankel function of the first kind $H_n^{(1)}(y) \equiv H_n(y)$:

$$g_n(r, r') = c_i J_n(\lambda_i r) + b_i H_n(\lambda_i r), \quad (4.8)$$

where

$$\lambda_i = \frac{\omega}{c} \sqrt{\varepsilon_i - c^2 k^2 / \omega^2}. \quad (4.9)$$

From the equation (3.4) it follows that the GF $\hat{G}_n^{(0)}(r, r')$ and its first derivative $\partial_r \hat{G}_n^{(0)}(r, r')$ are continuous at $r = r_i$ and, hence, the same holds for the functions $g_n(r, r')$. This gives the conditions

$$c_{i-1} J_n^{(l)}(\lambda_{i-1} r_i) + b_{i-1} H_n^{(l)}(\lambda_{i-1} r_i) = c_i J_n^{(l)}(\lambda_i r_i) + b_i H_n^{(l)}(\lambda_i r_i), \quad (4.10)$$

where $l = 0, 1$ and $h^{(0)}(r) = h(r)$, $h^{(1)}(r) = h'(r)$ for a given function $h(r)$. In the j -th layer we have

$$g_n(r, r') = \begin{cases} \bar{c}_j J_n(\lambda_j r) + \bar{b}_j H_n(\lambda_j r), & r_j < r < r' \\ c_j J_n(\lambda_j r) + b_j H_n(\lambda_j r), & r' < r < r_{j+1} \end{cases}. \quad (4.11)$$

The matching conditions at $r = r'$ read

$$\bar{c}_j J_n^{(l)}(\lambda_j r') + \bar{b}_j H_n^{(l)}(\lambda_j r') = c_j J_n^{(l)}(\lambda_j r') + b_j H_n^{(l)}(\lambda_j r') - \delta_{l1}/r', \quad (4.12)$$

again, with $l = 0, 1$. We have two additional conditions on the coefficients. The first one is the regularity condition on the axis z and gives $b_0 = 0$ for $r < r_0, r'$. The second condition requires traveling cylindrical waves propagating to the infinity and requires $c_N = 0$ for $r > r', r_N$. Hence, the number of the coefficients in the expressions for the functions $g_n(r, r')$ is equal to $2N + 2$. The conditions (4.10) and (4.12) provide $2N + 2$ equations to determine those coefficients.

From the conditions (4.10) and for $i \neq j$ the following recurrence relations are obtained between the coefficients:

$$\begin{aligned} c_i &= \frac{\pi}{2i} \left(c_{i-1} V_{(i)n}^{JH} + b_{i-1} V_{(i)n}^{HH} \right), \\ b_i &= -\frac{\pi}{2i} \left(c_{i-1} V_{(i)n}^{JJ} + b_{i-1} V_{(i)n}^{HJ} \right), \end{aligned} \quad (4.13)$$

where we have defined

$$V_{(i)n}^{FG} = F_n(\lambda_{i-1} r_i) r_i \partial_{r_i} G_n(\lambda_i r_i) - G_n(\lambda_i r_i) r_i \partial_{r_i} F_n(\lambda_{i-1} r_i), \quad (4.14)$$

for given functions $F_n(y)$ and $G_n(y)$. By using the recurrence relations for the Bessel functions, we also have

$$V_{(i)n}^{FG} = p r_i [\lambda_{i-1} F_{n+p}(\lambda_{i-1} r_i) G_n(\lambda_i r_i) - \lambda_i F_n(\lambda_{i-1} r_i) G_{n+p}(\lambda_i r_i)], \quad (4.15)$$

for $p = \pm 1$. From the boundary condition at $r = r_j$ one finds

$$\begin{aligned} \bar{c}_j &= \frac{\pi}{2i} \left(c_{j-1} V_{(j)n}^{JH} + b_{j-1} V_{(j)n}^{HH} \right), \\ \bar{b}_j &= \frac{\pi i}{2} \left(c_{j-1} V_{(j)n}^{JJ} + b_{j-1} V_{(j)n}^{HJ} \right). \end{aligned} \quad (4.16)$$

From (4.12), the relations

$$c_j = \bar{c}_j + \frac{i\pi}{2} H_n(\lambda_j r'), \quad b_j = \bar{b}_j - \frac{i\pi}{2} J_n(\lambda_j r'), \quad (4.17)$$

are obtained for the coefficients in the region $r_j < r < r_{j+1}$. Note that for $i \neq j$ we can also obtain the recurrence relations of the form

$$\begin{aligned} c_{i-1} &= \frac{\pi i}{2} \left[c_i V_{(i)n}^{HJ} + b_i V_{(i)n}^{HH} \right], \\ b_{i-1} &= \frac{\pi}{2i} \left[c_i V_{(i)n}^{JJ} + b_i V_{(i)n}^{JH} \right]. \end{aligned} \quad (4.18)$$

Combining the formulas (4.13) and (4.18), the relation

$$V_{(i)n}^{HJ} V_{(i)n}^{JH} - V_{(i)n}^{JJ} V_{(i)n}^{HH} = \frac{4}{\pi^2} \quad (4.19)$$

is obtained for the functions (4.14).

For $r_j < r' < r_{j+1}$ and $j \geq 1$, from the regularity condition in the region $r < r_1$ we have $b_0 = 0$. From the relations (4.13) and (4.16) it follows that all the coefficients c_i and b_i with $i < j$ and \bar{c}_j and \bar{b}_j are determined by c_0 : $c_i = C_i^{(\text{in})} c_0$, $b_i = B_i^{(\text{in})} c_0$, $\bar{c}_i = \bar{C}_i^{(\text{in})} c_0$, and $\bar{b}_i = \bar{B}_i^{(\text{in})} c_0$. Here, the coefficients $C_i^{(\text{in})}$ and $B_i^{(\text{in})}$ are uniquely determined in terms of the functions (4.14). In a similar manner, from the condition of traveling wave in the region $r > r_N$ we have $c_N = 0$ and, from the relations (4.18), all the coefficients c_i and b_i with $i \geq j$ are expressed in terms of b_N as $c_i = C_i^{(\text{out})} b_N$ and $b_i = B_i^{(\text{out})} b_N$. The coefficients c_0 and b_N are determined from the relations (4.17).

5 GF for a cylindrical waveguide immersed in a homogeneous medium

Now, let us specify the general procedure described above for the simple case of an inhomogeneous medium with a single boundary ($N = 1$) at $r = r_1$. This corresponds to a waveguide with a dielectric permittivity $\varepsilon_0(\omega)$ that is immersed in a homogeneous medium with a permittivity $\varepsilon_1(\omega)$. Two cases should be distinguished. For $0 < r' < r_1$, in the region $r < r_1$ we have $\bar{b}_0 = 0$, and b_0 is determined from (4.17) with $j = 0$. In the region $r > r_1$ one has the function (4.8) with $i = 1$ and $c_1 = 0$. c_0 is determined from the first relation (4.13) with $i = 1$, and b_1 is determined from the second relation in (4.13). The expression for b_1 is further simplified by using the relation (4.19). The final expression for the function $g_n(r, r')$ in the case $r' < r_1$ reads

$$g_n(r, r') = \begin{cases} \frac{i\pi}{2} \left[\frac{V_n^{HH}}{V_n^{JH}} J_n(\lambda_0 r_>) - H_n(\lambda_0 r_>) \right] J_n(\lambda_0 r_<), & r < r_1 \\ \frac{J_n(\lambda_0 r')}{V_n^{JH}} H_n(\lambda_1 r), & r > r_1 \end{cases}, \quad (5.1)$$

where $r_> = \max(r, r')$ and $r_< = \min(r, r')$, and we used the simplified notation $V_n^{FG} \equiv V_{(1)n}^{FG}$ with $V_{(1)n}^{FG}$ defined by (4.14). For the region $r' < r_1$ one has $b_0 = c_1 = 0$ and from the relations given above we get

$$g_n(r, r') = \begin{cases} \frac{H_n(\lambda_1 r')}{V_n^{JH}} J_n(\lambda_0 r), & r < r_1 \\ \frac{i\pi}{2} \left[\frac{V_n^{JJ}}{V_n^{JH}} H_n(\lambda_1 r_<) - J_n(\lambda_1 r_<) \right] H_n(\lambda_1 r_>), & r > r_1 \end{cases}. \quad (5.2)$$

The expressions for the functions $g_{n\pm 1}(r, r')$ are obtained from (5.1) and (5.2) by the replacements $n \rightarrow n \pm 1$.

With the functions (5.1) and (5.2), the GF $\hat{G}_n^{(0)}(r, r')$ is given by (4.7). The GF for a dielectric cylinder is obtained from the general formula (3.17) with $s = 1$ and $\hat{G}_n^{(1)}(r, r') = \hat{G}_n(r, r')$:

$$\hat{G}_n(r, r') = \hat{G}_n^{(0)}(r, r') + \frac{\hat{G}_n^{(0)}(r, r_1)\hat{S}(r_1, r')}{1 - \text{Sp } \hat{S}(r_1, r_1)}, \quad (5.3)$$

where $\hat{S}(r_1, r') = \hat{S}_1(r_1, r')$ and

$$\hat{S}(r_1, r') = r_1 \frac{\varepsilon_1^2 - \varepsilon_0^2}{2\varepsilon_0\varepsilon_1} \hat{D}(r) \hat{G}_n^{(0)}(r, r')|_{r=r_1}. \quad (5.4)$$

From the structure of the operator $\hat{D}(r)$, for the matrix elements of the product $\hat{D}(r)\hat{G}_n^{(0)}(r, r')$ we have $(\hat{D}(r)\hat{G}_n^{(0)}(r, r'))_{il} = 0$ for $i = 2, 3$. The nonzero elements of the first row in the region $r' > r_1$ are expressed as

$$\left(\hat{D}(r)\hat{G}_n^{(0)}(r, r')\right)_{1l}|_{r=r_1} = \frac{1}{2} J_n(\lambda_0 r_1) \left(\lambda_0 \sum_p \frac{p H_{n+p}(\lambda_1 r')}{V_{n+p}^{JH}}, i \lambda_0 \sum_p \frac{H_{n+p}(\lambda_1 r')}{V_{n+p}^{JH}}, 2ik \frac{H_n(\lambda_1 r')}{V_n^{JH}} \right), \quad (5.5)$$

and for $r' < r_1$ we have

$$\left(\hat{D}(r)\hat{G}_n^{(0)}(r, r')\right)_{1l}|_{r=r_1} = \frac{1}{2} H_n(\lambda_1 r_1) \left(\lambda_1 \sum_p \frac{p J_{n+p}(\lambda_0 r')}{V_{n+p}^{JH}}, i \lambda_1 \sum_p \frac{J_{n+p}(\lambda_0 r')}{V_{n+p}^{JH}}, 2ik \frac{J_n(\lambda_0 r')}{V_n^{JH}} \right), \quad (5.6)$$

where $l = 1, 2, 3$ and $\sum_p = \sum_{p=\pm 1}$. By using (4.15), the representation

$$V_{n+p}^{JH} = pr_1 [\lambda_1 J_{n+p}(\lambda_0 r_1) H_n(\lambda_1 r_1) - \lambda_0 J_n(\lambda_0 r_1) H_{n+p}(\lambda_1 r_1)], \quad (5.7)$$

is obtained for the combination of the Bessel and Hankel functions in (5.5) and (5.6).

By taking into account that $\text{Sp } \hat{S}(r_1, r_1) = S_{11}(r_1, r_1)$, we get

$$1 - \text{Sp } \hat{S}(r_1, r_1) = \frac{\varepsilon_1^2 - \varepsilon_0^2}{2\varepsilon_0\varepsilon_1} \alpha_n(\lambda_{01}, \lambda_{11}), \quad (5.8)$$

where the function

$$\alpha_n(k) = \frac{\varepsilon_0}{\varepsilon_1 - \varepsilon_0} - \frac{\lambda_{01}}{2} J_n(\lambda_{01}) \sum_{l=\pm 1} l \frac{H_{n+l}(\lambda_{11})}{V_{n+l}^{JH}} \quad (5.9)$$

is introduced with the notations

$$\lambda_{i1} = \lambda_i r_1, \quad i = 0, 1. \quad (5.10)$$

With the expressions given above, the GF is obtained from (5.3).

Let us introduce the function $G^{(c)}(r, r')$ in accordance with

$$\hat{G}^{(c)}(r, r') = \begin{cases} \hat{G}(r, r'), & (r - r_1)(r' - r_1) < 0 \\ \hat{G}(r, r') - \hat{G}_{\varepsilon_i}(r, r'), & (r - r_1)(r' - r_1) > 0 \end{cases}, \quad (5.11)$$

where $G_{\varepsilon_i}(r, r')$ is the GF for a homogeneous medium with permittivity ε_i . The latter is given by

$$\hat{G}_{\varepsilon_i}(r, r') = \frac{1}{2} \begin{pmatrix} \sum_p g_{n+p}^{(0)} & i \sum_p p g_{n+p}^{(0)} & 0 \\ -i \sum_p p g_{n+p}^{(0)} & \sum_p g_{n+p}^{(0)} & 0 \\ 0 & 0 & 2g_n^{(0)} \end{pmatrix}, \quad (5.12)$$

with the function

$$g_n^{(0)} = g_n^{(0)}(\lambda_i r, \lambda_i r') = \frac{\pi}{2i} J_n(\lambda_i r_<) H_n(\lambda_i r_>). \quad (5.13)$$

where, as before, $r_> = \max(r, r')$ and $r_< = \min(r, r')$. In (5.11), $\varepsilon_i = \varepsilon_0$ for $r < r_1$ and $\varepsilon_i = \varepsilon_1$ for $r > r_1$. For $r, r' > r_1$ we have $\hat{G}^{(c)}(r, r') = \hat{G}(r, r') - \hat{G}_{\varepsilon_1}(r, r')$ and $\hat{G}^{(c)}(r, r')$ presents the contribution to the GF in the exterior region due to the presence of a dielectric cylinder with permittivity ε_0 . Similarly, for $r, r' < r_1$, the function $\hat{G}^{(c)}(r, r')$ in the interior regions is interpreted as the part of the GF which comes from the replacement $\varepsilon_0 \rightarrow \varepsilon_1$ in the region $r > r_1$. It can be seen that, similar to the function (5.12), one has

$$G_{3l}(r, r') = 0, \quad l = 1, 2, \quad (5.14)$$

in both exterior and interior regions. We give the expressions for the nonzero components of the GF $\hat{G}^{(c)}(r, r')$ inside and outside the waveguide separately.

5.1 GF inside the cylinder

In the region inside the cylinder, $r < r_1$, we obtain

$$G_{lm}^{(c)}(r, r') = \frac{(-i)^{\delta_{m3}}}{2} \sum_p (ip)^{m-l} C_n^{(mp)} \frac{J_{n+p}(\lambda_0 r)}{V_{n+p}^{JH}}, \quad (5.15)$$

for $l = 1, 2$ and $m = 1, 2, 3$. Here, the coefficients are defined by

$$\begin{aligned} C_n^{(mp)} &= H_{n+p}(\lambda_1 r') + \frac{\lambda_{01} J_n(\lambda_{01})}{2p^{m-1} \alpha_n(k)} H_{n+p}(\lambda_{11}) \sum_{l=\pm 1} \frac{H_{n+l}(\lambda_1 r')}{l^m V_{n+l}^{JH}}, \quad r' > r_1, \\ C_n^{(mp)} &= \frac{i\pi}{2} V_{n+p}^{HH} J_{n+p}(\lambda_0 r') + \frac{\lambda_{11} H_n(\lambda_{11})}{2p^{m-1} \alpha_n(k)} H_{n+p}(\lambda_{11}) \sum_{l=\pm 1} \frac{J_{n+l}(\lambda_0 r')}{l^m V_{n+l}^{JH}}, \quad r' < r_1, \end{aligned} \quad (5.16)$$

for $m = 1, 2$, and

$$C_n^{(3p)} = \frac{kr_1 H_{n+p}(\lambda_{11})}{\alpha_n(k) V_n^{JH}} J_n(\lambda_0 r'_{1<}) H_n(\lambda_1 r'_{1>}), \quad (5.17)$$

where $r'_{1>} = \max(r_1, r')$ and $r'_{1<} = \min(r_1, r')$. For the remaining nonzero components one gets

$$\begin{aligned} G_{33}^{(c)}(r, r') &= H_n(\lambda_1 r') \frac{J_n(\lambda_0 r)}{V_n^{JH}}, \quad r' > r_1, \\ G_{33}^{(c)}(r, r') &= \frac{i\pi}{2} \frac{V_n^{HH}}{V_n^{JH}} J_n(\lambda_0 r') J_n(\lambda_0 r), \quad r' < r_1. \end{aligned} \quad (5.18)$$

In these expressions,

$$V_n^{FG} = \lambda_{11} F_n(\lambda_{01}) G'_n(\lambda_{11}) - \lambda_{01} G_n(\lambda_{11}) F'_n(\lambda_{01}), \quad (5.19)$$

with $F, G = J, H$ and V_{n+l}^{JH} is given by (5.7).

5.2 GF outside the cylinder

Outside the cylinder, $r > r_1$, the components with $l = 1, 2$ and $m = 1, 2, 3$ are expressed as

$$G_{lm}^{(c)}(r, r') = \frac{(-i)^{\delta_{m3}}}{2} \sum_p (ip)^{m-l} C_n^{(mp)} \frac{H_{n+p}(\lambda_1 r)}{V_{n+p}^{JH}}, \quad (5.20)$$

with the coefficients

$$\begin{aligned} C_n^{(mp)} &= \frac{i\pi}{2} V_{n+p}^{JJ} H_{n+p}(\lambda_1 r') + \frac{\lambda_{01} J_n(\lambda_{01})}{2p^{m-1} \alpha_n(k)} J_{n+p}(\lambda_{01}) \sum_{l=\pm 1} \frac{H_{n+l}(\lambda_1 r')}{l^m V_{n+l}^{JH}}, \quad r' > r_1, \\ C_n^{(mp)} &= J_{n+p}(\lambda_0 r') + \frac{\lambda_{11} H_n(\lambda_{11})}{2p^{m-1} \alpha_n(k)} J_{n+p}(\lambda_{01}) \sum_{l=\pm 1} \frac{J_{n+l}(\lambda_0 r')}{l^m V_{n+l}^{JH}}, \quad r' < r_1, \end{aligned} \quad (5.21)$$

for $m = 1, 2$, and

$$C_n^{(3p)} = \frac{k r_1 J_{n+p}(\lambda_{01})}{\alpha_n(k) V_n^{JH}} J_n(\lambda_0 r'_{1<}) H_n(\lambda_1 r'_{1>}). \quad (5.22)$$

The 33-component is given by the expressions

$$\begin{aligned} G_{33}^{(c)}(r, r') &= \frac{i\pi}{2} \frac{V_n^{JJ}}{V_n^{JH}} H_n(\lambda_1 r') H_n(\lambda_1 r), \quad r' > r_1, \\ G_{33}^{(c)}(r, r') &= \frac{J_n(\lambda_0 r')}{V_n^{JH}} H_n(\lambda_1 r), \quad r' < r_1, \end{aligned} \quad (5.23)$$

with the definition (5.19).

The formulas given above for the components of the GF apply to the general case of dielectric permittivities in separate media. In particular, the given expressions can be used to obtain the corresponding results for waveguides with conducting walls. For example, taking the formal limit $\varepsilon_N \rightarrow \infty$, we get the expressions for the electromagnetic GF inside a conducting cylindrical waveguide with radius r_N filled with cylindrically layered dielectric medium with permittivities $\varepsilon_0, \varepsilon_1, \dots, \varepsilon_{N-1}$.

6 General features of radiation processes

Having the GF, the Fourier components of the vector and scalar potentials are found by using the relations (2.16) and (2.18). Then, expanding the strengths $\mathbf{E}(x)$ and $\mathbf{B}(x)$ of the electric and magnetic fields

$$\left\{ \begin{array}{c} \mathbf{E}(x) \\ \mathbf{B}(x) \end{array} \right\} = \sum_{n=-\infty}^{+\infty} \int_{-\infty}^{+\infty} dk \int_{-\infty}^{+\infty} d\omega \left\{ \begin{array}{c} \mathbf{E}_n(k, \omega, r) \\ \mathbf{B}_n(k, \omega, r) \end{array} \right\} e^{in\phi + ikz - i\omega t}, \quad (6.1)$$

the Fourier components are obtained from the standard formulas $\mathbf{H}(x) = \nabla \times \mathbf{A}(x)$ and $\mathbf{E}(x) = -(1/c) \partial_t \mathbf{A}(x) - \nabla \varphi$. The obtained expressions for the electromagnetic fields are valid for general case of complex dielectric permittivities $\varepsilon_i(\omega)$.

In the idealized case of real functions $\varepsilon_i(\omega)$, the Fourier components of the GF may have poles for real values of k (on the integration axis in the Fourier expansion). These poles correspond to the normal modes (eigenmodes) of the dielectric cylinder and they are roots of the equation

$$\alpha_n(k) = 0. \quad (6.2)$$

By taking into account that

$$V_n^{JH} = \lambda_{11} J_n(\lambda_{01}) H'_n(\lambda_{11}) - \lambda_{01} H_n(\lambda_{11}) J'_n(\lambda_{01}), \quad (6.3)$$

the equation (6.2) is written as

$$\left(\lambda_0 \frac{H'_n}{H_n} - \lambda_1 \frac{J'_n}{J_n} \right) \left(\varepsilon_1 \lambda_0 \frac{H'_n}{H_n} - \varepsilon_0 \lambda_1 \frac{J'_n}{J_n} \right) = \frac{n^2 k^2 \omega_n^2}{c^2 r_1^2 \lambda_1^2 \lambda_0^2} (\varepsilon_1 - \varepsilon_0)^2, \quad (6.4)$$

where $H_n = H_n(\lambda_{11})$, $J_n = J_n(\lambda_{01})$, and the prime stands for the derivative of the function with respect to the argument. For real ε_i , the quantities λ_{i1}^2 are real and the right-hand side of (6.4) is real. The equation (6.4) determines the dispersion relation $\omega = \omega(k)$ for waves with a given n . It can be shown that for $\lambda_1^2 > 0$ the equation (6.4) has no solutions. The radial dependence of the corresponding Fourier modes is described by the Hankel functions $H_n(\lambda_1 r)$ and they describe the radiation propagating in the exterior medium $r > r_1$ at large distances from the waveguide.

For modes with $\lambda_1^2 < 0$, the radial dependence is given in terms of the modified Bessel function $K_n(\gamma_1 r)$ and the corresponding fields exponentially decay at large distances from the cylinder. Here and below, we use the notations

$$\gamma_i^2 = k^2 - \omega^2 \varepsilon_i / c^2, \quad \gamma_{i1} = \gamma_i r_1, \quad i = 0, 1. \quad (6.5)$$

In this case the equation for the eigenmodes (6.4) is written as (see, for example, [77]),

$$U_n(k) \equiv V_n \left(\varepsilon_1 \lambda_{01} \frac{K'_n}{K_n} + \varepsilon_0 \gamma_{11} \frac{J'_n}{J_n} \right) - \frac{n^2 k^2 \omega_n^2}{c^2 \gamma_1^2 \lambda_0^2} (\varepsilon_1 - \varepsilon_0)^2 = 0, \quad (6.6)$$

where $K_n = K_n(\gamma_{11})$ and the notation

$$V_n = \lambda_{01} \frac{K'_n}{K_n} + \gamma_{11} \frac{J'_n}{J_n} \quad (6.7)$$

is introduced. With these notations, the function (5.9) is presented in the form

$$\alpha_n(k) = \frac{U_n(k)}{(\varepsilon_1 - \varepsilon_0)(V_n^2 - n^2 u^2)}, \quad u = \frac{\lambda_0}{\gamma_1} + \frac{\gamma_1}{\lambda_0}. \quad (6.8)$$

The equation (6.6) describes two classes of modes. The first one corresponds to $\lambda_0^2 > 0$ and the radial dependence inside the cylinder is expressed in terms of the Bessel function $J_n(\lambda_0 r)$. These modes present the guided modes of a dielectric cylinder.

For the second class of modes one has $\lambda_0^2 < 0$ and the radial dependence inside the cylinder is described by the modified Bessel function $I_n(\gamma_0 r)$. These modes are localized near the surface of the waveguide and correspond to the surface polaritonic degrees of freedom. An important example of surface polaritons are surface plasmon polaritons [78, 79, 80]. They present collective oscillations of electron subsystem coupled to electromagnetic field and propagating along an interface between two media. Due to important properties, such as high density of electromagnetic energy and the possibility of concentrating electromagnetic fields beyond the diffraction limit of light waves, surface polaritons have found applications in a wide range of fundamental and applied fields. The latter include plasmonic waveguides, light-emitting devices, surface imaging, plasmonic solar cells, etc.

The equation for surface polaritonic eigenmodes, localized near a cylindrical surface, is obtained from (6.6) by passing to the modified Bessel function (see also [81, 82]):

$$\left(\frac{I'_n}{\gamma_0 I_n} - \frac{K'_n}{\gamma_1 K_n} \right) \left(\frac{\varepsilon_0 I'_n}{\gamma_0 I_n} - \frac{\varepsilon_1 K'_n}{\gamma_1 K_n} \right) = \frac{n^2 k^2 \omega_n^2}{r_1^2 c^2 \gamma_1^4 \gamma_0^4} (\varepsilon_1 - \varepsilon_0)^2, \quad (6.9)$$

with $I_n = I_n(\gamma_{01})$. By taking into account that $I'_n/I_n > n/\gamma_{01}$ and $K'_n/K_n < -n/\gamma_{11}$, it can be shown that the equation (6.9) has no solutions if the dielectric permittivities ε_0 and ε_1 have the same sign. This corresponds to the well-known condition for the presence of a surface polaritonic mode at the interface between two media: the dielectric permittivities of the neighboring media must have opposite signs within the considered spectral range.

As mentioned above, for real ε_i and for waves propagating at large distances from the cylinder (corresponding to $\lambda_1^2 > 0$), the function $\alpha_n(k)$ has no zeros within the integration range of the Fourier expansions (6.1). Mathematically, this is related to the fact that for $\lambda_1^2 > 0$ this function is a complex

function and it is not possible to have zero real and imaginary parts simultaneously. However, as discussed in [31, 38] for special cases of the charge motion, under certain conditions, at the zeros of the real part of the function $\alpha_n(k)$ the imaginary part can be exponentially small. This can lead to strong, narrow peaks in the angular distribution of the radiation intensity at large distances from the cylinder. We will consider this possibility in detail for the general case of charge motion.

From Debye's asymptotic expansion for the cylinder functions with large values of the order, $n \gg 1$, and for $|y| < 1$, one has [83]

$$\frac{J_n(ny)}{Y_n(ny)} \sim \frac{\operatorname{sgn} y}{2} e^{-2n\zeta(y)}, \quad \zeta(y) = \ln \frac{1 + \sqrt{1 - y^2}}{|y|} - \sqrt{1 - y^2}, \quad (6.10)$$

where $Y_n(u)$ is the Neumann function. By taking into account that this ratio is exponentially small, for the function $\alpha_n(k)$ in the range

$$0 < \frac{\omega^2}{c^2} \varepsilon_1 < n^2 + k^2 \quad (6.11)$$

(this corresponds to the condition $|y| < 1$ in (6.10)) we can write

$$\alpha_n(k) \approx \alpha_n^{(0)}(\lambda_{01}, \lambda_{11}) - \frac{i}{2} \lambda_{01} J_n(\lambda_{01}) \sum_{l=\pm 1} l \frac{Y_{n+l}(\lambda_{11})}{V_{n+l}^{JY}} \left[\frac{V_{n+l}^{JJ}}{V_{n+l}^{JY}} - \frac{J_{n+l}(\lambda_{11})}{Y_{n+l}(\lambda_{11})} \right], \quad (6.12)$$

where

$$\alpha_n^{(0)}(k) = \frac{\varepsilon_0}{\varepsilon_1 - \varepsilon_0} - \frac{\lambda_{01}}{2} J_n(\lambda_{01}) \sum_{l=\pm 1} l \frac{Y_{n+l}(\lambda_{11})}{V_{n+l}^{JY}}. \quad (6.13)$$

The function $\alpha_n^{(0)}(k)$ is real and it may have zeros. At these zeros and for large values of n , the function $\alpha_n(k)$ is approximated by the last term in (6.12) and it is suppressed by the factor $e^{-2n\zeta(\lambda_{11}/n)}$. This suggests that the intensity of radiation propagating in the exterior medium may have strong peaks at the zeros of $\alpha_n^{(0)}(k)$.

To clarify the existence of solutions to the equation $\alpha_n^{(0)}(k) = 0$, it is convenient to present it in the form

$$\left(\lambda_0 \frac{Y'_n}{Y_n} - \lambda_1 \frac{J'_n}{J_n} \right) \left(\lambda_0 \frac{\varepsilon_1 Y'_n}{\varepsilon_0 Y_n} - \lambda_1 \frac{J'_n}{J_n} \right) = \frac{n^2}{r_1^2} \left(1 - \frac{\lambda_0^2}{\lambda_1^2} \right) \left(\frac{\lambda_1^2}{\lambda_0^2} - \frac{\varepsilon_1}{\varepsilon_0} \right), \quad (6.14)$$

where $Y_n = Y_n(\lambda_{11})$. This equation is obtained from (6.4) by the replacement $H_n \rightarrow Y_n$. The different form of the right-hand side is convenient for the analysis. From the uniform asymptotic expansions of the cylinder functions for large values of the order n one has

$$\frac{J'_n(ny)}{J_n(ny)} \sim -\frac{Y'_n(ny)}{Y_n(ny)} \sim \frac{\sqrt{1 - y^2}}{y}, \quad (6.15)$$

in the range $0 < y < 1$, and

$$\frac{J'_n(ny)}{J_n(ny)} \sim -\tan \left[n\zeta_1(y) - \frac{\pi}{4} \right] \frac{\sqrt{y^2 - 1}}{y}, \quad (6.16)$$

for $y > 1$, with $\zeta_1(y) = \sqrt{y^2 - 1} - \operatorname{arcsec} y$. In the region $\omega^2 \varepsilon_0 < k^2 c^2$, the ratio J'_n/J_n is replaced by $-i I'_n/I_n$, $I_n = I_n(\gamma_{11})$, and the corresponding leading asymptotic reads

$$\frac{I'_n(ny)}{I_n(ny)} \sim \frac{\sqrt{1 + y^2}}{y}, \quad y > 0. \quad (6.17)$$

By using these asymptotics, it can be shown that for large n the equation (6.14) has a solution only under the condition

$$\frac{\omega^2}{c^2} \varepsilon_0 > \frac{n^2}{r_1^2} + k^2. \quad (6.18)$$

Now, combining this with (6.11), as a necessary condition, we get $\varepsilon_0 > \varepsilon_1$. Of course, the existence of solutions to (6.14) not necessarily mean that peaks will appear in the radiation intensity. In addition to the factor $1/\alpha_n^{(0)}(k)$, other factors in the corresponding formula can offset the contribution of this part. An example of the appearance of strong peaks will be considered below.

7 Electromagnetic fields for a charge circulating around a cylinder

As an application of the general setup described above, we consider the radiation generated by a charged particle moving with constant velocity v along a circular trajectory of radius $r = r_0 > r_1$. For the charge and current densities we have

$$j_i = \rho v_i = \frac{\delta_{2i}}{r} qv \delta(r - r_0) \delta(\phi - \omega_0 t) \delta(z), \quad (7.1)$$

where q is the charge of the particle and $\omega_0 = v/r_0$ is the angular velocity of the rotation.

7.1 Vector and scalar potentials

Substituting the Fourier component

$$j_{i,n}(k, \omega, r) = \frac{\delta_{2i}}{(2\pi)^2} \frac{qv}{r} \delta(r - r_0) \delta(\omega - n\omega_0), \quad (7.2)$$

in (2.16), for the vector potential we get

$$A_{i,n}(k, \omega, r) = -\frac{qv}{\pi c} G_{i2,n}(k, \omega, r, r_0) \delta(\omega - n\omega_0). \quad (7.3)$$

In this formula, the delta function is related to the periodic motion of the radiation source. It is also present in the Fourier components of the scalar potential and the field strengths. For a field $X(x)$ with the Fourier component $X_n(k, \omega, r)$, we define $X_n(k, r)$ in accordance with $X_n(k, \omega, r) = X_n(k, r) \delta(\omega - n\omega_0)$. The presence of the delta function allows to write the Fourier expansions (2.15) and (6.1) in the form

$$\begin{aligned} X(x) &= \sum_{n=-\infty}^{+\infty} \int_{-\infty}^{+\infty} dk X_n(k, r) e^{in(\phi - \omega_0 t) + ikz} \\ &= \operatorname{Re} \left[\sum_{n=0}^{\infty} (2 - \delta_{0n}) \int_{-\infty}^{+\infty} dk X_n(k, r) e^{in(\phi - \omega_0 t) + ikz} \right], \end{aligned} \quad (7.4)$$

for $X = \varphi, \mathbf{A}, \mathbf{E}, \mathbf{B}$. For real functions $X(x)$, we have the relation $X_n^*(k, r) = X_{-n}(-k, r)$ and we have used it in the second line. In particular, for the vector potential we have

$$A_{i,n}(k, r) = -\frac{qv}{\pi c} G_{i2,n}(k, n\omega_0, r, r_0). \quad (7.5)$$

By taking into account that $G_{32,n}(k, \omega, r, r') = 0$, we conclude that $A_{3,n}(k, r) = 0$. The expressions for nonzero components of the vector potential are obtained by using the formulas for the components of the GF given above.

We denote the fields and their Fourier images in the region with dielectric permittivity ε_j , $j = 0, 1$, by $X(x) = X^{(j)}(x)$ and $X_n^{(j)}(k, r)$, respectively. With such an arrangement, the functions $X_n^{(0)}(k, r)$ and $X_n^{(1)}(k, r)$ correspond to the fields in the regions $r < r_0$ and $r > r_0$. Then, the corresponding vector potentials are presented in a combined form

$$A_{m,n}^{(j)}(k, r) = A_{m,n}^{(\varepsilon_1)}(k, r) \delta_{1j} + \frac{qv}{2\pi c} \sum_p \frac{C_{(j)n}^{(p)}}{(ip)^m} Z_{n+p}^{(j)}(\lambda_j r), \quad (7.6)$$

where $m = 1, 2$,

$$\lambda_j^2 = \frac{\omega_n^2}{c^2} \varepsilon_j - k^2, \quad \omega_n = |n| \omega_0, \quad (7.7)$$

and we use the notation

$$Z_\nu^{(j)}(y) = \begin{cases} J_\nu(y), & j = 0 \\ H_\nu(y), & j = 1 \end{cases}. \quad (7.8)$$

In (7.6),

$$A_{m,n}^{(\varepsilon_j)}(k, r) = -\frac{iqv}{4c} \sum_p (-ip)^m J_{n+p}(\lambda_j r_{0<}) H_{n+p}(\lambda_j r_{0>}), \quad (7.9)$$

with $r_{0>} = \max(r_0, r)$ and $r_{0<} = \min(r_0, r)$, corresponds to the Fourier component of the vector potential generated by an orbiting charge in a homogeneous medium with dielectric permittivity ε_j . The coefficients $C_{(j)n}^{(p)}$ are expressed in terms of $C_n^{(2p)}$, given above, as

$$C_{(j)n}^{(p)} = \frac{C_n^{(2p)}}{V_{n+p}^{JH}}|_{r'=r_0, \omega=\omega_n}, \quad (7.10)$$

for the region with dielectric permittivity ε_j . Here, $C_n^{(2p)}$ in the exterior and interior regions are given by the first lines of (5.16) and (5.21). The explicit expressions read

$$C_{(j)n}^{(p)} = \frac{H_{n+p}(\lambda_1 r_0)}{V_{n+p}^{JH}} \left\{ \begin{array}{l} 1 \\ \frac{i\pi}{2} V_{n+p}^{JJ} \end{array} \right\} + \frac{p\lambda_{01} J_n(\lambda_{01})}{2\alpha_n(k)} \sum_{l=\pm 1} \frac{H_{n+l}(\lambda_1 r_0)}{V_{n+p}^{JH} V_{n+l}^{JH}} \left\{ \begin{array}{l} H_{n+p}(\lambda_{11}) \\ J_{n+p}(\lambda_{01}) \end{array} \right\}, \quad (7.11)$$

where the first and second lines correspond to $j = 0$ and $j = 1$, respectively, and λ_j is defined by (7.7). The modes with $n = 0$ are static and do not contribute to the radiation fields. In what follows, the presentation will be given for $n \neq 0$.

The Fourier components of the scalar potential inside and outside the cylinder are found from the relation

$$\varphi_n^{(j)}(k, r) = \frac{c}{\omega \varepsilon_j} \left\{ \frac{n}{r} A_{2,n}^{(j)}(k, r) - \frac{i}{r} \partial_1 \left[r A_{1,n}^{(j)}(k, r) \right] \right\}. \quad (7.12)$$

By taking into account that

$$\frac{1}{r} \partial_r \left[r Z_{n+p}^{(j)}(\lambda r) \right] = p \lambda Z_n^{(j)}(\lambda r) - \frac{pn}{r} Z_{n+p}^{(j)}(\lambda r), \quad (7.13)$$

for the functions (7.8), we get

$$\varphi_n^{(j)}(k, r) = \varphi_n^{(\varepsilon_1)}(k, r) \delta_{1j} - \frac{qv \lambda_j}{2\pi n \omega_0 \varepsilon_j} \sum_p C_{(j)n}^{(p)} Z_n^{(j)}(\lambda_j r). \quad (7.14)$$

Here,

$$\varphi_n^{(\varepsilon_j)}(k, r) = \frac{iqv \lambda_j}{2\omega_n \varepsilon_j} \begin{cases} J'_n(\lambda_j r_0) H_n(\lambda_j r) & r > r_0 \\ H'_n(\lambda_j r_0) J_n(\lambda_j r) & r < r_0 \end{cases} \quad (7.15)$$

corresponds to the scalar potential in a homogeneous medium with permittivity ε_j .

7.2 Electric and magnetic fields

Having the potentials, we turn to the magnetic and electric fields. The magnetic field is found from the relation $\mathbf{B} = \nabla \times \mathbf{A}$. By using the expressions for the Fourier component of the vector potential, the corresponding formulas for the magnetic field read

$$\begin{aligned} B_{m,n}^{(j)}(k, r) &= B_{m,n}^{(\varepsilon_1)}(k, r)\delta_{1j} + \frac{iqvk}{2\pi c} \sum_p \frac{C_{(j)n}^{(p)}}{(ip)^{m-1}} Z_{n+p}^{(j)}(\lambda_j r), \quad m = 1, 2, \\ B_{3,n}^{(j)}(k, r) &= B_{3,n}^{(\varepsilon_1)}(k, r)\delta_{1j} - \frac{qv\lambda_j}{2\pi c} \sum_p p C_{(j)n}^{(p)} Z_n^{(j)}(\lambda_j r), \end{aligned} \quad (7.16)$$

with $j = 0, 1$ and $m = 1, 2$. The electric field strength is found using the expressions for the potentials, or Maxwell's equation relating it to $\nabla \times \mathbf{B}$. For the Fourier components this gives

$$\begin{aligned} E_{m,n}^{(j)}(k, r) &= E_{m,n}^{(\varepsilon_1)}(k, r)\delta_{1j} + \frac{i^{1-m}qv}{4\pi\omega_n\varepsilon_j} \sum_{p,l=\pm 1} p^m Z_{n+p}^{(j)}(\lambda_j r) \left(l \frac{\omega_n^2}{c^2} \varepsilon_j + k^2 \right) C_{(j)n}^{(lp)}, \\ E_{3,n}^{(j)}(k, r) &= E_{3,n}^{(\varepsilon_1)}(k, r)\delta_{1j} + \frac{iqv\lambda_j k}{2\pi\omega_n\varepsilon_j} \sum_p C_{(j)n}^{(p)} Z_n^{(j)}(\lambda_0 r). \end{aligned} \quad (7.17)$$

As before, here $j = 0, 1$ and $m = 1, 2$. The given expressions are valid for general case of the dielectric permittivities dispersion. The expressions for the magnetic and electric fields $B_{m,n}^{(\varepsilon_j)}(k, r)$ and $E_{m,n}^{(\varepsilon_j)}(k, r)$ in a homogeneous medium with permittivity ε_j are obtained from the corresponding expressions for the second terms in (7.16) and (7.17) by the replacement $C_{(j)n}^{(p)} \rightarrow \pi J_{n+p}(\lambda_j r_0)/(2i)$ in the case $r > r_0$ and by the change $C_{(j)n}^{(p)} \rightarrow \pi H_{n+p}(\lambda_j r_0)/(2i)$ for $r < r_0$. Inside the cylinder we have $j = 0$ and the axial components of the electric and magnetic fields vanish on the cylinder axis, $B_{3,n}^{(0)}(k, 0) = E_{3,n}^{(0)}(k, 0) = 0$, $n \neq 0$.

8 Radiation at large distances from the cylinder

First we consider the radiation at large distances from the cylinder. As discussed above, it is determined by the modes for which $\omega^2\varepsilon_1 > c^2k^2$. The radial dependence of these modes is described by the Hankel function $H_n(\lambda_1 r)$ with $\lambda_1 > 0$ given by (7.7). At large distances from the cylinder, $\lambda_1 r \gg 1$, one has $H_n(y) \approx \sqrt{2/\pi}ye^{iy-n\pi/2-\pi/4}$, with $y = \lambda_1 r$, and the spacetime dependence of the Fourier components of the fields is given by $e^{i\lambda_1 r + ikz + in(\phi - \omega_0 t)}/\sqrt{r}$. These components describe radiation fields with angular frequency $\omega_n = |n|\omega_0$ propagating along the direction forming angle θ with respect to the axis z , determined from

$$k = \frac{\omega_n}{c} \sqrt{\varepsilon_1} \cos \theta. \quad (8.1)$$

The energy flux per unit time and through the cylindrical surface of radius r , averaged over the rotation period $T = 2\pi/\omega_0$, is given by

$$P = \frac{c}{2T} \int_0^T dt \int_{-\infty}^{\infty} dz r \mathbf{n}_r \cdot [\mathbf{E} \times \mathbf{B}], \quad (8.2)$$

where \mathbf{n}_r is the exterior unit vector normal to the integration surface. Substituting the Fourier expansions (7.4) we find

$$P = \pi r c \sum_{n=0}^{\infty} (2 - \delta_{0n}) \int_{-\infty}^{+\infty} dk \mathbf{n}_r \cdot \operatorname{Re} [\mathbf{E}_n(k, r) \times \mathbf{B}_n^*(k, r)]. \quad (8.3)$$

Taking the limit $r \rightarrow \infty$, one obtains

$$P = \frac{1}{4}q^2v^2 \sum_{n=1}^{\infty} \int \frac{dk}{\varepsilon_1 \omega_n} \left[\frac{\omega_n^2}{c^2} \varepsilon_1 \left| W_n^{(+1)} - W_n^{(-1)} \right|^2 + k^2 \left| W_n^{(+1)} + W_n^{(-1)} \right|^2 \right], \quad (8.4)$$

where the integration over k goes within the region $-\omega_n \sqrt{\varepsilon_1}/c < k < \omega_n \sqrt{\varepsilon_1}/c$ and the notation $W_n^{(p)} = J_{n+p}(\lambda_1 r_0) + 2iC_{(j)n}^{(p)}/\pi$ is introduced. The explicit expression reads

$$W_n^{(p)} = J_{n+p}(\lambda_1 r_0) - \frac{V_{n+p}^{JJ}}{V_{n+p}^{JH}} H_{n+p}(\lambda_1 r_0) + \frac{ip\lambda_{01} J_n(\lambda_{01})}{\pi\alpha_n(k)} \frac{J_{n+p}(\lambda_{01})}{V_{n+p}^{JH}} \sum_{l=\pm 1} \frac{H_{n+l}(\lambda_1 r_0)}{V_{n+l}^{JH}}. \quad (8.5)$$

Note that, from (4.15) with $i = 1$ and $F = J$, for the combinations of the Bessel and Hankel functions in (8.5) we have

$$V_{n+p}^{JG} = p [\lambda_{11} J_{n+p}(\lambda_{01}) G_n(\lambda_{11}) - \lambda_{01} J_n(\lambda_{01}) G_{n+p}(\lambda_{11})], \quad (8.6)$$

with $G = J, H$.

In (8.4), we can pass to the integration over the angle θ , $-\pi < \theta < \pi$, in accordance with (8.1). Introducing the average power radiated by the charge at a harmonic n into a unit solid angle, $dP_n/d\Omega$, in accordance with $P = \sum_{n=1}^{\infty} \int d\Omega (dP_n/d\Omega)$, where $d\Omega = \sin \theta d\theta d\phi$ is the solid angle element, we get (see also [23, 25])

$$\frac{dP_n}{d\Omega} = \frac{q^2 \beta^2 \omega_n^2 \sqrt{\varepsilon_1}}{8\pi c} \left[\left| W_n^{(1)} - W_n^{(-1)} \right|^2 + \left| W_n^{(1)} + W_n^{(-1)} \right|^2 \cos^2 \theta \right], \quad (8.7)$$

with $\beta = v/c$. The quantities in the arguments of the cylinder functions in (8.5) are expressed as

$$\lambda_0 = \frac{\omega_n}{c} \sqrt{\varepsilon_0 - \varepsilon_1 \cos^2 \theta}, \quad \lambda_1 = \frac{\omega_n}{c} \sqrt{\varepsilon_1} \sin \theta. \quad (8.8)$$

The formula (8.7) is valid for general case of complex dielectric function $\varepsilon_0 = \varepsilon_0(\omega)$. Note that, for a given angular velocity ω_0 , the dependence on the radius of the rotation orbit enters in the formula (8.7) via the Hankel functions $H_{n\pm 1}(\lambda_1 r_0)$. The spectral-angular density of the radiation for a charge circulating inside a cylinder has been studied in [31].

For $\varepsilon_0 = \varepsilon_1$ one has $W_n^{(p)} = J_{n+p}(\lambda_1 r_0)$ and from (8.7) we obtain the corresponding quantity for a charge circulating in a homogeneous medium with permittivity ε_1 (see, e.g., [2]):

$$\frac{dP_n^{(\varepsilon_1)}}{d\Omega} = \frac{q^2 \omega_n^2}{2\pi c \sqrt{\varepsilon_1}} [\beta^2 \varepsilon_1 J_n'^2(n\beta \sqrt{\varepsilon_1} \sin \theta) + \cot^2 \theta J_n^2(n\beta \sqrt{\varepsilon_1} \sin \theta)]. \quad (8.9)$$

Note that $\omega_n r_0 = nv$ and the spectral-angular density of the radiated power (8.7) has a functional structure

$$\frac{dP_n}{d\Omega} = \frac{f_n(\beta_1, r_1/r_0, \varepsilon_0/\varepsilon_1)}{r_0^2 \sqrt{\varepsilon_1}}, \quad \beta_1 = \frac{v}{c} \sqrt{\varepsilon_1} \quad (8.10)$$

This means that for fixed β_1 , the combination $\sqrt{\varepsilon_1} r_0^2 dP_n/d\Omega$ depends on r_1 and r_0 and on the dielectric permittivities in the form of the ratios r_1/r_0 and $\varepsilon_0/\varepsilon_1$. In the limit $r_1/r_0 \ll 1$, to the leading order, we get $dP_n/d\Omega \approx dP_n^{(\varepsilon_1)}/d\Omega$ and the contribution induced by the presence of the cylinder decays as $(r_1/r_0)^{2n}$. For a non-relativistic motion, $\beta \ll 1$, one has $dP_n/d\Omega \propto \beta^{2(n+1)}$ and the dominant contribution comes from the lowest harmonic $n = 1$. The radiation features for a charged particle circulating in a homogeneous medium are discussed in [2], [62]-[67], based on the formula (8.9). It has been shown that, under the Cherenkov condition $\beta_1 > 1$, the interference of synchrotron and Cherenkov radiations leads to interesting effects in both spectral and angular distributions of the radiation intensity.

According to the analysis in 6, narrow peaks appear when $\lambda_{11} < n < \lambda_{01}$. However, this is not sufficient. Other factors in (8.5) need to be estimated. As mentioned above, at the zeros of the function (6.13) one has $\alpha_n(k) \propto e^{-2n\zeta(\lambda_{11}/n)}$. Under the condition $\lambda_{01} > n$, which is necessary for the zeros of $\alpha_n^{(0)}(k)$, one has $V_{n+p}^{JH} \propto e^{n\zeta(\lambda_{11}/n)}$. From (8.5) it follows that, for the peaks to appear, one must have $\lambda_1 r_0 < n$, for which $H_{n+l}(\lambda_1 r_0) \propto e^{n\zeta(\lambda_1 r_0/n)}$. In this case, at the peaks $dP_n/d\Omega \propto e^{2n\zeta(\lambda_1 r_0/n)}$. Consequently, the conditions for the appearance of the peaks read $\lambda_1 r_0 < n < \lambda_{01}$. With the expressions (8.8), they are translated to

$$1 - \frac{c^2}{v^2 \varepsilon_1} < \cos^2 \theta < \frac{\varepsilon_0}{\varepsilon_1} \left(1 - \frac{c^2}{v_c^2 \varepsilon_0} \right), \quad (8.11)$$

where $v_c = r_1 \omega_0 = v r_1 / r_0$ is the velocity of the particle image on the cylinder surface. In particular, the conditions $\varepsilon_0 > \varepsilon_1$ and $v_c \sqrt{\varepsilon_0} > c$ should be obeyed. The latter relation states that the velocity of the charge image on the cylinder surface should obey the Cherenkov condition for the material of the cylinder.

Using the asymptotic expressions for cylinder functions allows us to estimate the widths of the peaks. By expanding the function $\alpha_n(k)$ in (8.5) near the peaks, it can be seen that the width of the peak is determined by the imaginary part of the function $\alpha_n(k)$, evaluated at the location of the peak. The width is of the order $e^{-2n\zeta(\lambda_{11}/n)}$. Note that the function $\zeta(y)$ is monotonically decreasing with increasing y and $\zeta(\lambda_{11}/n) > \zeta(\lambda_1 r_0/n)$. We have considered an idealized case in which the dielectric permittivities are real. In real situations, the increase in the peak height with increasing n is restricted by several factors. In particular, the imaginary parts of the permittivities contribute to the expansion of the function $\alpha_n(k)$ near the peaks, restricting the increase in height and decrease in width.

In the numerical examples we will consider the angular dependence of the the number of the radiated quanta per unit time and on a given harmonic, averaged over the rotation period. It is given by $dN_n/d\Omega = (\hbar\omega_n)^{-1} dP_n/d\Omega$. In Fig. 1, we display the angular distribution of the number of the radiated quanta (in units of $q^2/\hbar c$) during the rotation period $T = 2\pi/\omega_0$, given by

$$F_n(\theta) = T \frac{\hbar c}{q^2} \frac{dN_n}{d\Omega}. \quad (8.12)$$

The right panel corresponds to the radiation from a charge rotating in a vacuum ($\varepsilon_1 = 1$) around a cylinder with dielectric permittivity $\varepsilon_0 = 3.8$ (real part of the dielectric permittivity for fused silica). For the values of the other parameters we have taken $\beta = 0.98$, $r_1/r_0 = 0.95$, and the numbers near the curves correspond to the values of the harmonic n . The angular distribution is symmetric with respect to the plane $\theta = \pi/2$. For comparison, the left panel of Fig. 1 shows the corresponding quantity for the synchrotron radiation from a charge circulating in a vacuum ($\varepsilon_0 = \varepsilon_1 = 1$). We have verified that the locations of the peaks in the problem with a cylinder are given with high accuracy by zeros of the function (6.13). For example, the peak for the harmonic $n = 5$ with the height $F_n(\theta) \approx 8.4$ is located at $\theta \approx 0.78$ and the same approximate value is predicted by the equation (6.14). One has the same accuracy for the case $n = 10$ with the peaks at $\theta \approx 0.71$ and 1.13 . For the height of the peak at $\theta \approx 0.71$ one has $F_n(\theta) \approx 1.5$.

In the example of Fig. 1, the charge moves in a vacuum and this figure illustrates the influence of the dielectric cylinder on the characteristics of the synchrotron radiation. The right panel of Fig. 2 presents the case with a charge circulating in a medium with dielectric permittivity $\varepsilon_1 = 2.1$ (real part of dielectric permittivity for Teflon). The dielectric permittivity for the cylinder and the values of the other parameters are the same as those for Fig. 1. The graphs on the left panel correspond to the radiation in a homogeneous medium with permittivity ε_1 . Now, the Cherenkov condition in the exterior medium is satisfied, $\beta_1 > 1$, and the radiation outside the cylinder is a superposition of synchrotron and Cherenkov radiations. Again, we have checked that the positions of the peaks on the harmonics $n = 5, 10$ are determined by the roots of the equation (6.14). The height of the peak for $n = 5$ located at $\theta \approx 0.38$

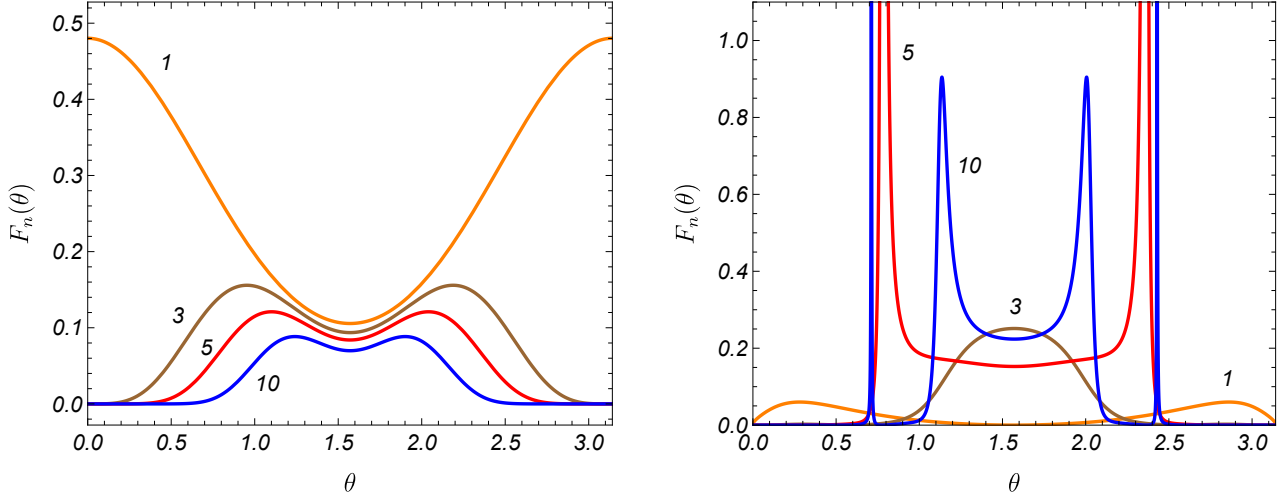


Figure 1: The angular density of the number of the radiated quanta per rotation period, in units of $q^2/\hbar c$, versus the angle θ , for different values of the radiation harmonic n (numbers near the curves). The left panel corresponds to the synchrotron radiation in a vacuum ($\epsilon_0 = \epsilon_1 = 1$) and the right panel presents the data for a charge rotating around a dielectric cylinder with permittivity $\epsilon_0 = 3.8$ ($\epsilon_1 = 1$). The graphs are plotted for $\beta = 0.98$, $r_1/r_0 = 0.95$.

is equal to ≈ 2.54 . For the radiation on the harmonic $n = 10$, the heights of the peaks at $\theta \approx 0.25$ and $\theta \approx 0.56$ are given by $F_n(\theta) \approx 4.8 \cdot 10^4$ and $F_n(\theta) \approx 29.8$, respectively. Of course, these data are for an idealized problem with real dielectric permittivities. As mentioned above, the imaginary parts of the permittivities will reduce the heights of the peaks. In the case of a particle rotating in a homogeneous medium ($\epsilon_0 = \epsilon_1$), the only nonzero contribution to the angular density of the radiation intensity in the limit $\theta \rightarrow 0$ comes from the mode $n = 1$. For a particle circulating around a cylinder ($\epsilon_0 \neq \epsilon_1$), we have $\lim_{\theta \rightarrow 0} dP_n/d\Omega = 0$ for all harmonics. This behavior is seen from the expression (8.5) in the limit $\lambda_1 \rightarrow 0$, corresponding to $\theta \rightarrow 0$. For a charge rotating in a homogeneous medium, the function $W_n^{(p)}$ is reduced to $J_{n+p}(\lambda_1 r_0)$ and the mode $n = 1$ with $p = -1$ gives a nonzero contribution in the limit at hand. In the problem with a dielectric cylinder, the last term in (8.5) tends to zero in the limit $\lambda_1 \rightarrow 0$ for all modes, and the contribution of the first term with the function $J_{n+p}(\lambda_1 r_0)$ is canceled by the second term.

The discussion in Section 6 showed that the condition $\epsilon_0 > \epsilon_1$ is necessary for peaks to appear. In Fig. 3, the function $F_n(\theta)$ is plotted for different values of n (numbers near the curves) and for $\epsilon_0 = 1$, $\epsilon_1 = 3.8$ (cylindrical hole in a dielectric medium). For the other parameters we have taken the same values as in Figs. 1 and 2. According to the analysis presented above, in this case the strong peaks in the angular distribution are absent.

We have considered numerical examples with a positive dielectric function of the cylinder. Formula (8.7) for the angular density of the radiation intensity is also valid in spectral ranges where the permittivity ϵ_0 becomes negative. The arguments given above for the presence of strong peaks in the angular distribution of the radiation intensity also apply in this case. The corresponding features of the spectral-angular distribution of the radiation at large distances from the cylinder have been discussed in [58].

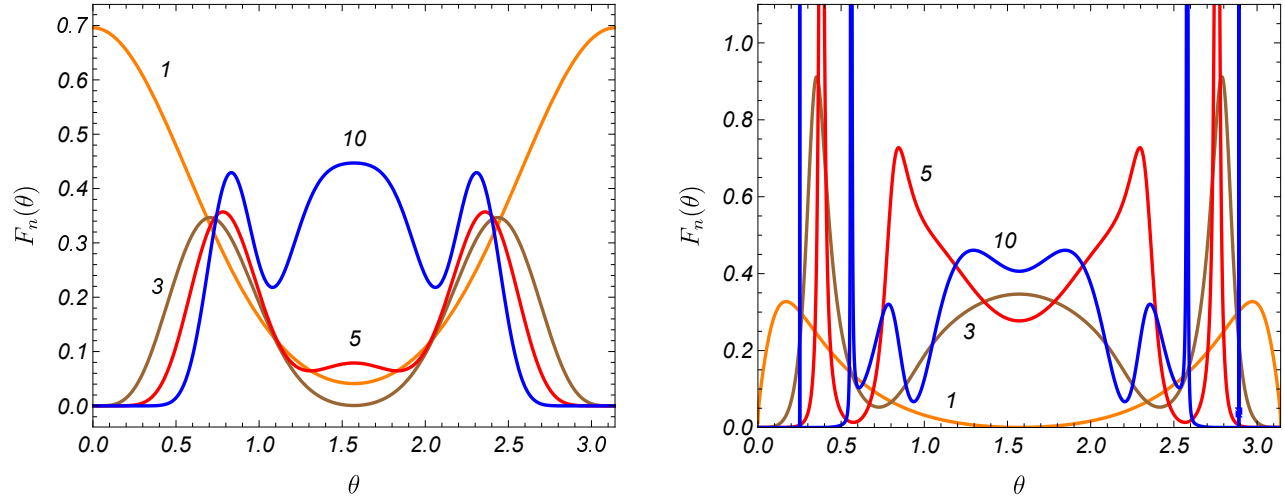


Figure 2: The same as in Fig. 1 for $\varepsilon_1 = 2.1$.

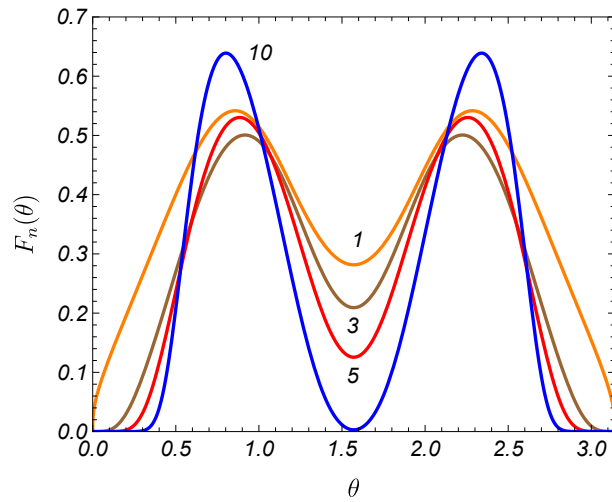


Figure 3: The same as on the right panel of Fig. 1 for $\varepsilon_0 = 1$, $\varepsilon_1 = 3.8$.

9 Radiation on the normal modes of a cylinder

9.1 Radiation fields

Now, let us consider the radiation in the spectral range where $\lambda_1^2 < 0$ and the radiation is confined inside the cylinder or near its surface. In order to separate the corresponding contributions to the total field, we consider the limit $z \rightarrow \infty$ in the expansion (7.4). The problem under consideration is symmetric with respect to the plane $z = 0$ and, without loss of generality, we can consider the half space $z > 0$. The phase of the exponent in the integrand of (7.4) has no stationary points. According to the stationary phase method, for regular functions $X_n(k, r)$ and for large z , the integral would decay exponentially. The radiation fields will come from possible singular points of the integrand. For the fields discussed in Section 7, the singularities are contained in the parts with the function $\alpha_n(k)$ and they are poles at the zeros of this function. As mentioned above, they present the eigenmodes of a cylindrical waveguide.

Let $\pm k_{n,s}$, $k_{n,s} > 0$, $s = 1, 2, \dots$, be the solutions of the equation (6.2) with respect to k for $n \neq 0$. For $\lambda_{11}^2 < 0$ the equation is transformed to the form (6.6). For the roots $k_{n,s}$ we introduce the notations

$$\lambda_{n,s}^{(0)} \equiv r_1 \sqrt{\omega_n^2 \varepsilon_0 / c^2 - k_{n,s}^2}, \quad \gamma_{n,s}^{(1)} \equiv r_1 \sqrt{k_{n,s}^2 - \varepsilon_1 \omega_n^2 / c^2}. \quad (9.1)$$

For real ε_j , $\gamma_{n,s}^{(1)}$ is positive, while $\lambda_{n,s}^{(0)}$ can be either positive or purely imaginary. For the evaluation of the radiation parts in the fields, we need to specify the integration contour in (7.4) near the poles $\pm k_{n,s}$. This is done introducing a small imaginary part of the dielectric permittivity, $\varepsilon_j = \varepsilon_j' + i\varepsilon_j''$, with $\varepsilon_j''(\omega) > 0$ for $\omega > 0$. On the base of this, it can be seen that (for details see, e.g., [48]) in the integral over k the contour should avoid the poles $k_z = k_{n,s}$ ($k_z = -k_{n,s}$) from below (above). With this specification and for $z > 0$, closing the integration contour by the large semicircle in the upper half-plane of complex variable k , the radiation fields are obtained with the help of the residue theorem:

$$X^{(r)}(x) = 4\pi \text{Re} \left\{ i \sum_{n=1}^{\infty} e^{in(\phi - \omega_0 t)} \sum_{s=1}^{s_n} \text{Res}_{k=k_{n,s}} \left[e^{ikz} X_n(k, r) \right] \right\}, \quad (9.2)$$

where the superscript (r) stands for the radiation parts of the fields. Note that the nonzero contributions to the residue come from the parts of the coefficients $C_{(j)n}^{(p)}$ containing the factor $1/\alpha_n(k)$.

Evaluating the residue, the radiation fields are presented in the form

$$X^{(r)}(x) = \frac{qv}{c} \sum_{n=1}^{\infty} \sum_{s=1}^{s_n} \frac{X_{n,s}(r)}{\alpha'_n(k_{n,s})} R[n(\phi - \omega_0 t) + k_{n,s} z], \quad (9.3)$$

where s_n is the number of the modes with given n , and

$$\alpha'_n(k_{n,s}) = \partial_k \alpha_n(k) |_{k=k_{n,s}}. \quad (9.4)$$

For the function determining the dependence on the spacetime coordinates (t, ϕ, z) one has $R(x) = \sin x$ for the components $X^{(r)} = E_1^{(r)}, B_2^{(r)}, B_3^{(r)}$ and $R(x) = \cos x$ for the components $X^{(r)} = E_2^{(r)}, E_3^{(r)}, B_1^{(r)}$.

The parts in the coefficients $C_{(j)n}^{(p)}$, giving the contributions to the radiation fields are expressed in terms of the function

$$U_{(j)n}^{(p)} = \frac{\lambda_{01} J_n(\lambda_{01})}{V_n^{JK}} \sum_{l=\pm 1} \frac{K_{n+l}(\gamma_1 r_0)}{V_{n+l}^{JK}} \begin{cases} K_{n+p}(\gamma_{11}), & j = 0 \\ J_{n+p}(\lambda_{01}), & j = 1 \end{cases}, \quad (9.5)$$

with the notation

$$\begin{aligned} V_n^{JK} &= J_n(\lambda_0 r_1) r_1 \partial_{r_1} K_n(\gamma_1 r_1) - K_n(\gamma_1 r_1) r_1 \partial_{r_1} J_n(\lambda_0 r_1) \\ &= p \lambda_{01} J_{n+p}(\lambda_{01}) K_n(\gamma_{11}) - \gamma_{11} J_n(\lambda_{01}) K_{n+p}(\gamma_{11}), \end{aligned} \quad (9.6)$$

where $p = \pm 1$. Note that we have the relation

$$V_{n+p}^{JK} = p J_n(\lambda_{01}) K_n(\gamma_{11}) (V_n - p n u), \quad (9.7)$$

with the function V_n from (6.7). For the modes with $\lambda_1^2 < 0$, the function (5.9) is written as

$$\alpha_n(k) = \frac{\varepsilon_0}{\varepsilon_1 - \varepsilon_0} - \frac{\lambda_{01}}{2} J_n(\lambda_{01}) \sum_{l=\pm 1} l \frac{K_{n+l}(\lambda_{11})}{V_{n+l}^{JK}}. \quad (9.8)$$

By using the properties of the Bessel functions and the equation $\alpha_n(k_{n,s}) = 0$ for the modes, the derivative of the function (9.8) at the roots $k = k_{n,s}$ is presented in the form

$$\begin{aligned} \alpha'_n(k) = & \frac{r_1^3 k}{2} \sum_{l=\pm 1} \left(\frac{J_n K_n}{V_{n+l}^{JK}} \right)^2 \left\{ \gamma_1 \frac{K_{n+l}}{K_n} \left[1 - \left(\frac{n+l}{\lambda_{01}} \right)^2 + \left(\frac{J'_n}{J_n} + \frac{1}{\lambda_{01}} \right)^2 \right] \right. \\ & \left. \times -l \lambda_0 \frac{J_{n+l}}{J_n} \left[1 + \left(\frac{n+l}{\gamma_{11}} \right)^2 - \left(\frac{K'_n}{K_n} + \frac{1}{\gamma_{11}} \right)^2 \right] \right\}_{k=k_{n,s}}. \end{aligned} \quad (9.9)$$

In the region $r < r_1$, the functions $X_{n,s}(r)$ for the components of the magnetic field read

$$\begin{aligned} B_{m,n,s}(r) &= -k \sum_p p^m U_{(0)n}^{(p)} J_{n+p}(\lambda_0 r) |_{k=k_{n,s}}, \\ B_{3,n,s}(r) &= \lambda_0 \sum_p U_{(0)n}^{(p)} J_n(\lambda_0 r) |_{k=k_{n,s}}, \end{aligned} \quad (9.10)$$

with $m = 1, 2$. For the electric field, by using the representations (7.17), we get

$$\begin{aligned} E_{m,n,s}(r) &= \frac{(-1)^m c}{2\omega_n \varepsilon_0} \sum_{p,l=\pm 1} p^{m-1} J_{n+p}(\lambda_0 r) \left(\frac{\omega_n^2 \varepsilon_0}{c^2} + lk^2 \right) U_{(0)n}^{(lp)} |_{k=k_{n,s}}, \\ E_{3,n,s}(r) &= -\frac{v \lambda_0 k}{n \omega_0 \varepsilon_0} \sum_p p U_{(0)n}^{(p)} J_n(\lambda_0 r) |_{k=k_{n,s}}. \end{aligned} \quad (9.11)$$

On the axis of the waveguide we have $B_{3,n,s}(0) = E_{3,n,s}(0) = 0$.

For the region outside the cylinder, $r > r_1$, the components of the magnetic field are expressed as

$$\begin{aligned} B_{m,n,s}(r) &= -k \sum_p p^m U_{(1)n}^{(p)} K_{n+p}(\gamma_1 r) |_{k=k_{n,s}}, \\ B_{3,n,s}(r) &= -\gamma_1 \sum_p p U_{(1)n}^{(p)} K_n(\gamma_1 r) |_{k=k_{n,s}}, \end{aligned} \quad (9.12)$$

and for the electric field we get

$$\begin{aligned} E_{m,n,s}(r) &= \frac{(-1)^m c}{2\omega_n \varepsilon_1} \sum_{p,l=\pm 1} p^{m-1} K_{n+p}(\gamma_1 r) \left(l \frac{\omega_n^2 \varepsilon_1}{c^2} + k^2 \right) U_{(1)n}^{(lp)} |_{k=k_{n,s}}, \\ E_{3,n,s}(r) &= \frac{c \gamma_1 k}{\omega_n \varepsilon_1} \sum_p U_{(1)n}^{(p)} K_n(\gamma_1 r) |_{k=k_{n,s}}, \end{aligned} \quad (9.13)$$

again, with $m = 1, 2$. For a given angular velocity ω_0 of the charge rotation, the fields depend on the orbit radius r_0 through the functions $K_{n\pm 1}(\gamma_1 r_0)$ in (9.5) and they monotonically decay with increasing r_0 .

The expressions given in this section describe the fields for both guided and surface polaritonic type modes. For guided modes, the arguments $\lambda_{01} = \lambda_{n,s}^{(0)}$ and $\lambda_0 r = \lambda_{n,s}^{(0)} r / r_1$ of the Bessel function $J_n(y)$ are real. For radiated surface polaritons, these arguments are purely imaginary with a positive imaginary part. In this case we introduce the modified Bessel function $I_n(y)$.

For guided modes we have

$$\varepsilon_1 < (ck/\omega_n)^2 < \varepsilon_0. \quad (9.14)$$

The dispersion $\omega = \omega(k)$ for those modes is determined from the equation (6.6). For waves radiated by a charge on a given harmonic n , the allowed values of k are determined by the intersection points of the dispersion curves $\omega = \omega(k)$ in the (k, ω) -plane with the horizontal line $\omega = n\omega_0$. The dependence of the radiation fields on the radius of the rotation orbit enters in the form of the functions $K_{n\pm 1}(\gamma_1 r_0)$ (see (9.5)) and these fields in both exterior and interior regions are suppressed by the factor $e^{-\gamma_1 r_0}$ for $\gamma_1 r_0 \gg 1$. The radiation is a result of medium polarization by the field of charged particle. For the spectral range corresponding to the guided modes, the Fourier components of the charge's field exponentially decay at large distances from the charge trajectory and the mentioned exponential suppression of the radiation intensity is a consequence of that behavior.

9.2 Radiation energy flux

Given the radiation fields, we can evaluate the radiation intensity on the eigenmodes of a dielectric cylinder. As a physical characteristic of the intensity we consider the energy flux per unit time through the plane $z = \text{const}$ at large distances from the radiation source. It is expressed in terms of the axial component of the Poynting vector and is given by

$$P^{(\text{nm})} = \frac{c}{4\pi} \int_0^\infty dr \int_0^{2\pi} d\phi r \left(E_1^{(\text{r})} B_2^{(\text{r})} - E_2^{(\text{r})} B_1^{(\text{r})} \right), \quad (9.15)$$

where (nm) stands for the normal modes. Plugging the radiation fields from (9.3), with the components $X_{m,n,s}(r)$ for the electric and magnetic fields from (9.10)-(9.13), it can be shown that the radial integrals are reduced to $\int_0^{r_1} dr r J_{n+p}^2(\lambda_0 r)$ and $\int_{r_1}^\infty dr r K_{n+p}^2(\gamma_1 r)$ in the interior and exterior regions, respectively. These integrals are evaluated by standard formulas [84].

Let us denote by $P_{jn}^{(\text{nm})}$, $j = 0, 1$, the energy flux on a fixed harmonic n in the medium with dielectric permittivity ε_j . After straightforward transformations and using the relation (9.7), for the energy flux inside the cylinder one gets

$$\begin{aligned} P_{0n}^{(\text{nm})} &= \frac{q^2 v^2 r_1^2}{8\omega_n \varepsilon_0} \sum_{s=1}^{s_n} \frac{k \lambda_{01}^2 J_n^2}{\alpha_n'^2(k_{n,s})} \left(\sum_{l'=\pm 1} \frac{K_{n+l'}(\gamma_1 r_0)}{V_{n+l'}^{JK}} \right)^2 \sum_{p,l=\pm 1} \frac{K_{n+p}}{V_{n+p}^{JK}} \\ &\quad \times \left(\frac{\omega_n^2 \varepsilon_0}{c^2} + lk^2 \right) \frac{K_{n+lp}}{V_{n+lp}^{JK}} \left[J_{n+p}^{\prime 2} + \left(1 - \left(\frac{n+p}{\lambda_{01}} \right)^2 \right) J_{n+p}^2 \right]. \end{aligned} \quad (9.16)$$

We remind that here $J_\nu = J_\nu(\lambda_{01})$ and $K_\nu = K_\nu(\gamma_{11})$ with $\nu = n, n \pm 1$. In a similar way, the energy flux in the exterior region, $r > r_1$, is presented in the form

$$\begin{aligned} P_{1n}^{(\text{nm})} &= \frac{q^2 v^2 r_1^2}{8\omega_n \varepsilon_1} \sum_{s=1}^{s_n} \frac{k \lambda_{01}^2 J_n^2}{\alpha_n'^2(k_{n,s})} \left(\sum_{l'=\pm 1} \frac{K_{n+l'}(\gamma_1 r_0)}{V_{n+l'}^{JK}} \right)^2 \sum_{p,l=\pm 1} \frac{J_{n+p}}{V_{n+p}^{JK}} \\ &\quad \times \left(k^2 + l \frac{\omega_n^2 \varepsilon_1}{c^2} \right) \frac{J_{n+lp}}{V_{n+lp}^{JK}} \left[K_{n+p}^{\prime 2} - \left(1 + \left(\frac{n+p}{\gamma_{11}} \right)^2 \right) K_{n+p}^2 \right]. \end{aligned} \quad (9.17)$$

Alternative representations are obtained by using the relations

$$\begin{aligned}\sum_{l=\pm 1} \left(k^2 + l \frac{\omega_n^2 \varepsilon_1}{c^2} \right) \frac{J_{n+l p}}{V_{n+l p}^{JK}} &= \frac{2 \varepsilon_1 \lambda_0}{r_1 (\varepsilon_0 - \varepsilon_1)} \frac{p V_n^{JK}}{K_n V_{n+p}^{JK}}, \\ \sum_{l=\pm 1} \left(\frac{\omega_n^2 \varepsilon_0}{c^2} + l k^2 \right) \frac{K_{n+l p}}{V_{n+l p}^{JK}} &= \frac{2 \varepsilon_0 \gamma_1}{r_1 (\varepsilon_1 - \varepsilon_0)} \frac{V_n^{JK}}{J_n V_{n+p}^{JK}},\end{aligned}\quad (9.18)$$

where $k = k_{n,s}$. They are obtained by taking into account the equation (6.6) with the roots $k_{n,s}$. With the relations (9.18), the energy fluxes are expressed as

$$\begin{aligned}P_{0n}^{(nm)} &= \frac{q^2 v^2}{4 \omega_n (\varepsilon_1 - \varepsilon_0)} \sum_{s=1}^{s_n} \frac{k \gamma_{11} \lambda_{01}^2 J_n V_n^{JK}}{\alpha_n'^2 (k_{n,s})} \left[\sum_{l=\pm 1} \frac{K_{n+l} (\gamma_1 r_0)}{V_{n+l}^{JK}} \right]^2 \\ &\quad \times \sum_{p=\pm 1} \frac{K_{n+p}}{(V_{n+p}^{JK})^2} \left[J_{n+p}^{\prime 2} + \left(1 - \left(\frac{n+p}{\lambda_{01}} \right)^2 \right) J_{n+p}^2 \right]_{k=k_{n,s}},\end{aligned}\quad (9.19)$$

inside the cylinder, $r < r_1$, and

$$\begin{aligned}P_{1n}^{(nm)} &= \frac{q^2 v^2}{4 \omega_n (\varepsilon_0 - \varepsilon_1)} \sum_{s=1}^{s_n} \frac{k \lambda_{01}^3 J_n^2 V_n^{JK}}{\alpha_n'^2 (k_{n,s}) K_n} \left[\sum_{l=\pm 1} \frac{K_{n+l} (\gamma_1 r_0)}{V_{n+l}^{JK}} \right]^2 \\ &\quad \times \sum_{p=\pm 1} \frac{p J_{n+p}}{(V_{n+p}^{JK})^2} \left[K_{n+p}^{\prime 2} - \left(1 + \left(\frac{n+p}{\gamma_{11}} \right)^2 \right) K_{n+p}^2 \right]_{k=k_{n,s}},\end{aligned}\quad (9.20)$$

in the exterior region, $r > r_1$. We note that the expressions in the square brackets in the second lines of (9.19) and (9.20) are obtained from the radial integrals involving the functions $J_{n+p}^2(\lambda_0 r)$ and $K_{n+p}^2(\gamma_1 r)$, and they are positive.

9.3 Total energy flux and the radiated power

Having the energy fluxes inside and outside the cylinder, the total energy flux through the plane $z = \text{const}$, for the radiation on a given harmonic, is obtained as the sum of these two contributions:

$$P_n^{(nm)} = P_{0n}^{(nm)} + P_{1n}^{(nm)}. \quad (9.21)$$

Combining the expressions (9.19) and (9.20) we get

$$\begin{aligned}P_n^{(nm)} &= \frac{q^2 v^2}{4 \omega_n (\varepsilon_1 - \varepsilon_0)} \sum_{s=1}^{s_n} \frac{k \lambda_{01}^2 J_n V_n^{JK}}{\alpha_n'^2 (k_{n,s}) K_n} \left(\sum_{l=\pm 1} \frac{K_{n+l} (\gamma_1 r_0)}{V_{n+l}^{JK}} \right)^2 \\ &\quad \times \sum_{p=\pm 1} \left\{ \gamma_{11} \frac{K_n K_{n+p}}{(V_{n+p}^{JK})^2} \left[J_{n+p}^{\prime 2} + \left(1 - \left(\frac{n+p}{\lambda_{01}} \right)^2 \right) J_{n+p}^2 \right] \right. \\ &\quad \left. - \lambda_{01} \frac{p J_n J_{n+p}}{(V_{n+p}^{JK})^2} \left[K_{n+p}^{\prime 2} - \left(1 + \left(\frac{n+p}{\gamma_{11}} \right)^2 \right) K_{n+p}^2 \right] \right\}_{k=k_{n,s}}.\end{aligned}\quad (9.22)$$

Using the properties of the Bessel function and by taking into account the expression (9.9) for the derivative of the function $\alpha_n(k)$ at the roots $k_{n,s}$, it can be shown that the sum over p is equal to $2\alpha_n'(k_{n,s})/(r_1^2 k_{n,s})$. This leads to the formula

$$P_n^{(nm)} = \frac{q^2 v^2}{2 \omega_n (\varepsilon_1 - \varepsilon_0)} \sum_{s=1}^{s_n} \frac{\lambda_{01}^2 J_n V_n^{JK}}{\alpha_n'(k) K_n} \left[\sum_{l=\pm 1} \frac{K_{n+l} (\gamma_1 r_0)}{V_{n+l}^{JK}} \right]^2_{k=k_{n,s}}. \quad (9.23)$$

Let us compare the total energy flux with the radiated power $W^{(\text{nm})}$ expressed in terms of the work per unit time done by the radiation field on the charge:

$$W^{(\text{nm})} = - \int_0^\infty dr \int_0^{2\pi} d\phi \int_{-\infty}^\infty dz r \mathbf{j} \cdot \mathbf{E}^{(\text{r})}. \quad (9.24)$$

For the current density (7.1), the component $E_2^{(\text{r})}(x)$ of the electric field is required, evaluated at $r = r_0$. Plugging the representation (9.3) for this component, by taking into account (9.13) for $m = 2$ and the first relation in (9.18), for the radiated power on n -th harmonic we get

$$W_n^{(\text{nm})} = \frac{q^2 v^2}{\omega_n (\varepsilon_1 - \varepsilon_0)} \sum_{s=1}^{s_n} \frac{\lambda_0^2 J_n V_n^{JK}}{\alpha'_n(k_{n,s}) K_n} \left[\sum_{l=\pm 1} \frac{K_{n+l}(\gamma_1 r_0)}{V_{n+l}^{JK}} \right]_{k=k_{n,s}}^2. \quad (9.25)$$

Comparing with (9.23), we see that $W_n^{(\text{nm})} = 2P_n^{(\text{nm})}$. Here the factor 2 takes into account the energy fluxes in the regions $z > 0$ and $z < 0$. For real ε_j the absorption is absent and we could expect this energy balance. For a given angular velocity ω_0 , the energy fluxes and the radiated power are monotonically decreasing functions of the rotation orbit radius r_0 and decay as $e^{-2\gamma_1 r_0}$ for $\gamma_1 r_0 \gg 1$. An alternative expression for the radiated power in the form of guided modes is given in [55]. The equivalence to a simpler representation (9.25) can be seen by using the first relation in (9.18). The energy fluxes and the radiated power for guided modes generated by a point charge rotating inside a cylindrical waveguide are investigated in [48].

For numerical analysis of the radiated power in the form of guided modes, we have considered an example with dielectric permittivities $\varepsilon_0 = 3.8$ and $\varepsilon_1 = 1$, and with the parameters $\beta = 0.9, 0.95, 0.98$, $r_1/r_0 = 0.95$. For these values of the parameters and for $\beta = 0.98$, one has $s_n = 1$ for $n = 1, \dots, 7$, $s_n = 2$ for $n = 8, \dots, 13$, $s_n = 3$ for $n = 14, \dots, 17$, and so on. In the case $\beta = 0.95$ ($\beta = 0.9$), the radiation is absent on the harmonics $n = 2, 3$ ($n = 2, 3, 4$), $s_n = 1$ for $n = 1, 4, \dots, 8$ ($n = 1, 5, \dots, 8$), and $s_n = 2$ for $n = 9, \dots, 17$. In Fig. 4, we have plotted the total flux of the number of quanta for guided modes, radiated per rotation period, versus the harmonic number. The numbers near the plot markers correspond to the values of β . The corresponding values for $k_{n,s}$ lie in the range (9.14). As seen from Fig. 4, the radiation intensity essentially increases with the appearance of a new mode $k_{n,s}$ for a given n . This happens on the mode $n = 8$ for $\beta = 0.98$, and on the mode $n = 9$ for $\beta = 0.9, 0.95$.

10 Radiation of surface polaritons

The formulas given above for the radiation on the normal modes of a dielectric waveguide are valid for both guided and surface polaritonic modes. For convenience of the further use, this section presents the formulas for the characteristics of the radiated surface polaritons and describes their radiation features. Various methods are used to excite surface polaritons. These include prism and grating coupling, guided photonic modes of waveguide, focused optical and electron beams (see [45, 78, 79, 80, 85, 86]).

For surface polaritons, the quantity λ_0 is purely imaginary and the corresponding formulas for the radiation energy fluxes from a charge rotating around a dielectric cylinder are obtained from the expressions given above by the substitutions $\lambda_0 = i\gamma_0$ and $J_n(\lambda_0 r) = e^{in\pi/2} I_n(\lambda_0 r)$. The energy flux through the plane $z = \text{const}$ in the region $r < r_1$ reads

$$\begin{aligned} P_{0n}^{(\text{sp})} &= \frac{q^2 v^2}{4\omega_n (\varepsilon_1 - \varepsilon_0)} \sum_{s=1}^{s_n} \frac{k\gamma_{11}\gamma_{01}^2 I_n V_n^{IK}}{\alpha'^2_n(k_{n,s})} \left[\sum_{l=\pm 1} \frac{K_{n+l}(\gamma_1 r_0)}{l V_{n+l}^{IK}} \right]^2 \\ &\times \sum_{p=\pm 1} \frac{K_{n+p}}{(V_{n+p}^{IK})^2} \left[\left(1 + \left(\frac{n+p}{\gamma_{01}} \right)^2 \right) I_{n+p}^2 - I_{n+p}^2 \right]_{k=k_{n,s}}, \end{aligned} \quad (10.1)$$

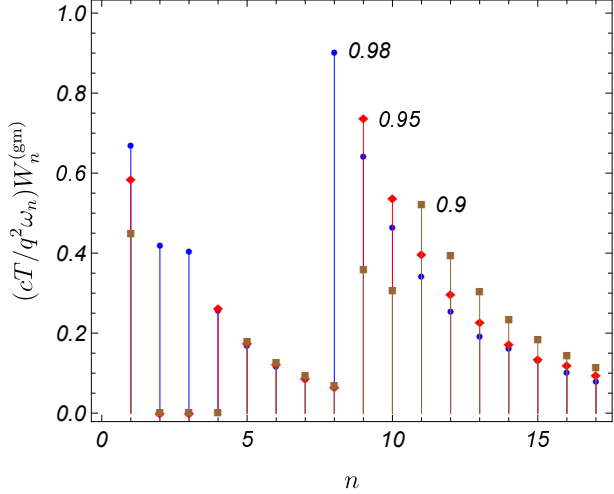


Figure 4: The number of the radiated quanta per rotation period in the form of guided modes (in units of $q^2/\hbar c$) versus of the radiation harmonic. The numbers near the curves correspond to the values of β . For the remaining parameters we have taken $\varepsilon_0 = 1$, $\varepsilon_1 = 3.8$, and $r_1/r_0 = 0.95$.

where $I_\nu = I_\nu(\gamma_{01})$, $K_\nu = K_\nu(\gamma_{11})$, $\nu = n, n \pm 1$, and

$$V_n^{IK} = \gamma_{11} I_n K'_n - \gamma_{01} K_n I'_n = -\gamma_{01} I_{n+p} K_n - \gamma_{11} I_n K_{n+p}, \quad (10.2)$$

for $p = \pm 1$. Note that the latter function is always negative. For the energy flux outside the cylinder, $r > r_1$, one obtains

$$\begin{aligned} P_{1n}^{(\text{sp})} &= \frac{q^2 v^2}{4\omega_n(\varepsilon_0 - \varepsilon_1)} \sum_{s=1}^{s_n} \frac{k \gamma_{01}^3 I_n^2 V_n^{IK}}{\alpha_n'^2(k_{n,s}) K_n} \left[\sum_{l=\pm 1} \frac{K_{n+l}(\gamma_1 r_0)}{l V_{n+l}^{IK}} \right]^2 \\ &\times \sum_{p=\pm 1} \frac{I_{n+p}}{(V_{n+p}^{IK})^2} \left[K_{n+p}^{l2} - \left(1 + \left(\frac{n+p}{\gamma_{11}} \right)^2 \right) K_{n+p}^2 \right]_{k=k_{n,s}}. \end{aligned} \quad (10.3)$$

The functions in the square brackets of (10.1) and (10.3) under the sign of the summation over p are obtained from the radial integrals $\int_0^{r_1} dr r I_{n+p}^2(\gamma_0 r)$ and $\int_{r_1}^\infty dr r K_{n+p}^2(\gamma_0 r)$, and they are positive. Hence, the signs of the energy fluxes are determined by the sign of the ratio $V_n^{IK}/(\varepsilon_1 - \varepsilon_0)$. By taking into account that $V_n^{IK} < 0$, we conclude that

$$(\varepsilon_0 - \varepsilon_1) P_{1n}^{(\text{sp})} < 0 < (\varepsilon_0 - \varepsilon_1) P_{0n}^{(\text{sp})}. \quad (10.4)$$

In particular, this shows that the energy fluxes for surface polaritons have opposite signs inside and outside the cylinder. We recall that for the presence of surface polaritons the permittivities ε_0 and ε_1 should have opposite signs. Combining this with (10.4), we conclude that the energy flux is positive/negative in a medium with positive/negative dielectric permittivity.

The total energy flux for radiated surface polaritons is expressed as

$$P_n^{(\text{sp})} = \frac{q^2 v^2}{2\omega_n(\varepsilon_1 - \varepsilon_0)} \sum_{s=1}^{s_n} \frac{\gamma_0^2 I_n V_n^{IK}}{\alpha_n'(k_{n,s}) K_n} \left[\sum_{l=\pm 1} \frac{K_{n+l}(\gamma_1 r_0)}{l V_{n+l}^{IK}} \right]_{k=k_{n,s}}^2. \quad (10.5)$$

For the radiated power $W^{(\text{sp})}$ of the surface polaritons we have $W_n^{(\text{sp})} = 2P_n^{(\text{sp})}$. The radiated power was investigated in [53] by evaluating the work done by the radiation field on a charged particle. The explicit expression of the derivative $\alpha'_n(k_{n,s})$ in the formulas (10.1)-(10.5) reads

$$\begin{aligned} \alpha'_n(k) = & -\frac{r_1^3 k}{2} \sum_{l=\pm 1} \left(\frac{I_n K_n}{V_{n+l}^{IK}} \right)^2 \left\{ \gamma_1 \frac{K_{n+l}}{K_n} \left[1 + \left(\frac{n+l}{\gamma_{01}} \right)^2 - \left(\frac{I'_n}{I_n} + \frac{1}{\gamma_{01}} \right)^2 \right] \right. \\ & \left. + \gamma_0 \frac{I_{n+l}}{I_n} \left[1 + \left(\frac{n+l}{\gamma_{11}} \right)^2 - \left(\frac{K'_n}{K_n} + \frac{1}{\gamma_{11}} \right)^2 \right] \right\}_{k=k_{n,s}}. \end{aligned} \quad (10.6)$$

The dispersion relation $\omega = \omega(k)$ for surface polaritons is obtained from (6.9). In the problem under consideration, the values $k = k_{n,s}$ for the radiated surface polaritons are determined by the intersection points of the curve $\omega = \omega(k)$ and the line $\omega = \omega_n$ in the (k, ω) -plane. An equivalent form of the dispersion equation reads

$$\alpha_n(k) = \frac{\varepsilon_0}{\varepsilon_1 - \varepsilon_0} + \frac{1}{2} \sum_{l=\pm 1} \left(1 + \frac{\gamma_1 I_{n+l} K_n}{\gamma_0 I_n K_{n+l}} \right)^{-1} = 0. \quad (10.7)$$

For a given value of the combination $\beta_1 = \beta \sqrt{\varepsilon_1}$, the dimensionless product $k_{n,s} r_1$ is a function of n , r_1/r_0 , and $\varepsilon_0/\varepsilon_1$.

Let us consider the asymptotic properties of the radiated surface polaritonic modes. Unlike the guided modes, for surface polaritons with a given frequency ω_n , the values of the projection k of the wave vector are limited only from below. In the analysis of the radiated surface polariton modes it is convenient to introduce the dimensionless combination $z_n = kc/\omega_n$. This combination is the ratio of the light wavelength of angular frequency ω_n in the vacuum to the wavelength of surface polariton with the same frequency. For large values of k one has $z_n \gg 1$ and the arguments of the modified Bessel functions are large. By using the corresponding asymptotic formulas, in the leading order, the dispersion equation is reduced to

$$\alpha_n(k) \approx \frac{1}{\varepsilon_1/\varepsilon_0 - 1} + \frac{1}{\gamma_1/\gamma_0 + 1} = 0, \quad (10.8)$$

having the solution

$$k^2 \approx \frac{\omega_n^2}{c^2} \frac{\varepsilon_0 \varepsilon_1}{\varepsilon_0 + \varepsilon_1}. \quad (10.9)$$

Note that the dispersion relation $\omega = \omega(k)$ for surface polaritons on a planar boundary, separating media with dielectric permittivities ε_0 and ε_1 , is given by (10.9) with ω_n replaced by ω . Such an approximation by the dispersion relation for a flat boundary was expected, since the limit under consideration corresponds to small wavelengths, for which the curvature of the cylinder is not essential. In particular, the relation (10.9) shows that $\varepsilon_0 \rightarrow -\varepsilon_1$ in the limit $k \rightarrow \infty$.

The features caused by the curvature of the cylinder surface are important for wavelengths of the order of the cylinder radius and larger. To be specific, let us consider the case $\varepsilon_0 < 0 < \varepsilon_1$. With this choice, the minimal value of k is determined from the condition $\lambda_1^2 < 0$ and $k \geq \omega_n \sqrt{\varepsilon_1}/c$. For the values of k close to this lower limit, assuming that $\gamma_{11} \ll 1$, in (10.7) we replace the Macdonald function by its asymptotic for small values of the argument. In addition, one has $\gamma_{01} \approx (\omega_n r_1/c) \sqrt{|\varepsilon_0| + \varepsilon_1}$. For the lowest radiated harmonic $n = 1$, from the dispersion relation (10.7) we obtain

$$\alpha_1(k) \approx \frac{1}{1 - \varepsilon_0/\varepsilon_1} + \frac{I_0}{2\gamma_{01} I_1 \ln \gamma_{11}} = 0. \quad (10.10)$$

From here it follows that the modes with k close to the lower limit are radiated in the spectral range where $\varepsilon_0/\varepsilon_1 \ll -1$. The situation is completely different for the harmonics $n \geq 2$. In this case, under

the condition $\gamma_{11} \ll 1$, we find

$$\alpha_n(k) \approx \frac{1}{2} \left(\frac{1 + \varepsilon_0/\varepsilon_1}{1 - \varepsilon_0/\varepsilon_1} + \frac{I_n}{I_{n-2}} \right) = 0. \quad (10.11)$$

By taking into account that for $v_c|\varepsilon_0|/c \gg 1$ the argument of the modified Bessel functions is large and using the corresponding asymptotics, it can be shown that for modes $n > 1$ and in the region $|\varepsilon_0| \gg 1$ the equation (10.11) has no solutions. For a given $n \geq 2$ one has a threshold ε_{0n} for the cylinder dielectric permittivity and the equation (10.7) has no roots in the region $\varepsilon_0 < \varepsilon_{0n}$. When k tends to its lower limit $\omega_n \sqrt{\varepsilon_1}/c$, the dielectric permittivity ε_0 approaches to a finite value $\varepsilon_{0n}^{(1)}$. With increasing v_c/c , the limiting value $\varepsilon_{0n}^{(1)}$ tends to ε_{0n} .

The features described above for the distribution of the surface polariton modes are numerically illustrated in Fig. 5. In this analysis it is convenient to consider (10.7) as an equation with respect to ε_0 for a given value of $z_n = kc/\omega_n$. This dependence is plotted for $\varepsilon_1 = 1$, $r_1/r_0 = 0.95$, and for different values of β (the numbers near the curves). The left and right panels correspond to the harmonics $n = 1$ and $n = 2$, respectively. According to asymptotic analysis, in both cases we have $\varepsilon_0 \rightarrow -1$ in the limit $z_n \gg 1$. In the limit $z_n \rightarrow 1$, one has $\varepsilon_0 \rightarrow -\infty$ for $n = 1$ and $\varepsilon_0 \rightarrow \varepsilon_{0n}^{(1)}$ for $n = 2$. The limiting values are given by $\varepsilon_{0n}^{(1)} \approx -1.02, -1.12, -1.52, -3.41$ for $\beta = 0.1, 0.25, 0.5, 0.95$, respectively. As seen from the graphs, $\varepsilon_{0n}^{(1)} = \varepsilon_{0n}$ for $\beta = 0.5, 0.95$. For $\beta = 0.1, 0.25$ one has $\varepsilon_{0n} \approx -1.21, -1.23$. In the cases $\beta = 0.5, 0.95$ and for a given $\varepsilon_0 < -1$, there is a single root for $n = 1$ and a single root in the range $\varepsilon_{0n} < \varepsilon_0 < -1$ for $n = 2$. For $\beta = 0.1, 0.25$, depending on the value of ε_0 , one can have one, two or three roots.

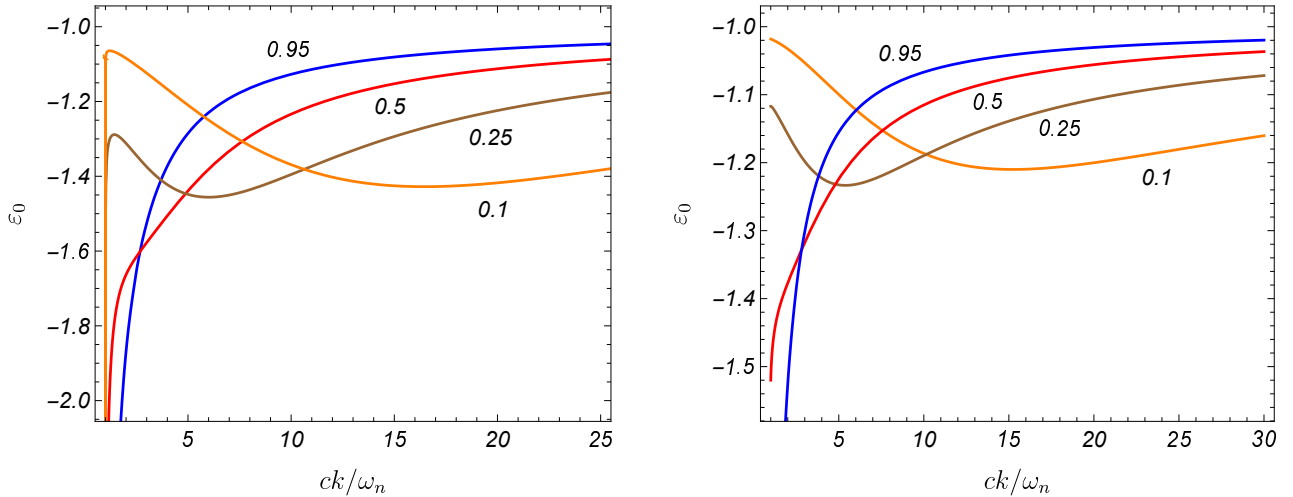


Figure 5: The surface polaritonic modes of a dielectric cylinder with respect to the ratio $z_n = kc/\omega_n$. The numbers near the curves are the values of β and the graphs are plotted for $n = 1$ (left panel) and $n = 2$ (right panel). We have taken $\varepsilon = 1$ for the exterior medium.

Figure 6 presents the number of the radiated quanta for surface polaritons per rotation period T (in units of $q^2/\hbar c$) as a function of ε_0 (left panel) and $z_n = kc/\omega_n$ (right panel), for $\varepsilon_1 = 1$, $r_1/r_0 = 0.95$, $\beta = 0.95$. The numbers near the curves present the values of n . The dependence z_n on the dielectric permittivity ε_0 for $n = 1, 2$ is given in Fig. 5. As seen, the number of the quanta radiated in the form of surface polaritons can be essentially larger than the one for guided modes.

The above discussion is presented without specifying the dispersion of the dielectric permittivities $\varepsilon_j = \varepsilon_j(\omega)$. The allowed values of $k_{n,s}$ for the normal modes of the cylinder, being the zeros of the

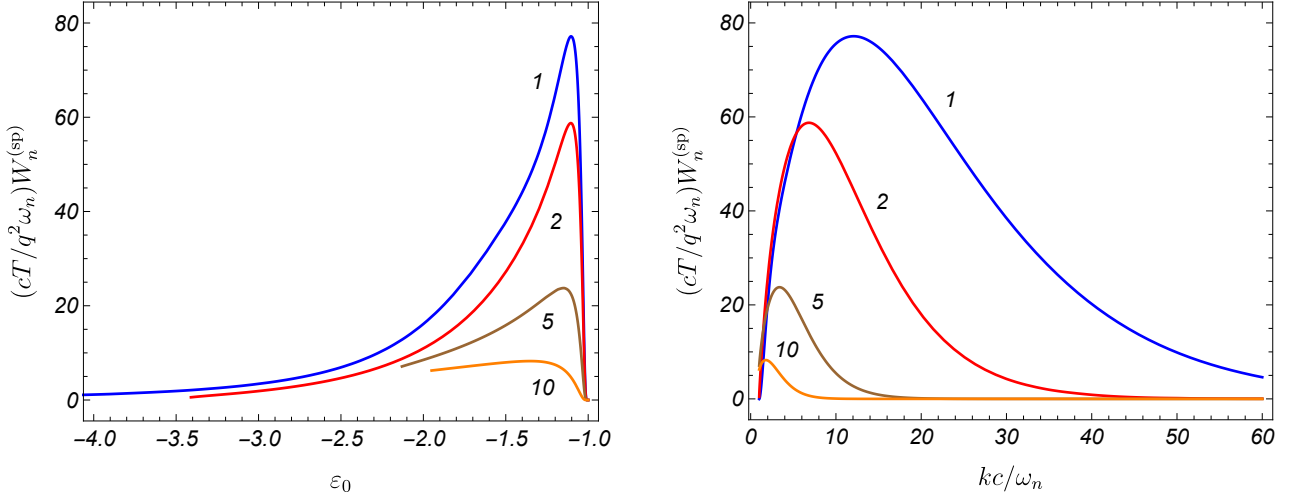


Figure 6: The number of the quanta, radiated per rotation period, in the form of surface polaritons (in units of $q^2/\hbar c$), as a function of the cylinder dielectric permittivity (left panel) and as a function of $z_n = kc/\omega_n$ (right panel). The numbers near the curves are the values of the radiated harmonic n . For the parameters we have taken $\epsilon_1 = 1$, $r_1/r_0 = 0.95$, $\beta = 0.95$.

function $\alpha_n(k)$, depend on specific dispersion law. For instance, in the case corresponding to the data in Fig. 5, the roots $k_{n,s}$ are obtained by solving the equation $\epsilon_0(\omega_n) = h_n(kc/\omega_n)$ with respect to k for a given ω_n . Here, the function $h_n(kc/\omega_n)$ is presented by the graphs in Fig. 5 for $n = 1$ and $n = 2$. As an example of dispersion, the Drude model can be considered with $\epsilon_0(\omega) = 1 - \omega_p^2/\omega^2$ with ω_p being the plasma frequency.

We considered the radiation of a charged particle rotating around a cylinder as an application of the GF with the components given in Section 5. Another class of problems employing different GF components is discussed in [57, 59, 60, 61]. These papers study the radiation of point particles and annular beams moving parallel to the axis of a dielectric cylinder.

11 Conclusion

We reviewed the features of radiation processes in a cylindrically symmetric medium. For given sources of the electromagnetic field, the response of the medium is encoded in the Green function. In cylindrical coordinates and for a medium with a dielectric function $\hat{\epsilon}(r)$, the equation for the GF is presented in the form (2.7) with matrix operators (2.5) and (2.6). In accordance with the problem's symmetry, it is convenient to switch to the partial Fourier representation (2.9). Given a current density $\mathbf{j}(r)$, the Fourier component of the vector potential can be found using the relation (2.16). Section 3 considers the special case of a cylindrically symmetric medium consisting of N homogeneous cylindrical layers described by dielectric function (3.1). The equation for the corresponding GF is transformed to the form (3.2) with a set of delta-type "potentials" $\hat{A}^{(s)}(r)$ located at separating boundaries and defined by (3.3). Presenting the equation for the GF in the form of Lipmann-Schwinger equation, the relation (3.17) is derived for intermediate GFs $\hat{G}_n^{(s)}(r, r')$ defined by (3.6). For $s = N$, this function coincides with the GF for N layers and the equation (3.17) provides a recurrence relation to find the function $\hat{G}_n^{(N)}(r, r')$ having the GF $\hat{G}_n^{(N-1)}(r, r')$ for $N - 1$ layers.

Using the recurrence relation (3.17), we reduce the problem to the determining the GF $G_n^{(0)}(r, r')$ being the solution of the equation (3.4). In Section 4, we diagonalized this equation by transformation

(4.1). The diagonal components of the transformed GF are found by solving the corresponding equation in separate layers and imposing matching conditions at the interfaces between them. By imposing the regularity condition on the symmetry axis and the radiation condition in the exterior medium, one gets $2N+2$ equations for the $2N+2$ coefficients. They are expressed in terms of the functions (4.14) with $F_n(y)$ and $G_n(y)$ being the Bessel and Hunkel functions, respectively. The initial GF $G_n^{(0)}(r, r')$ is obtained via inverse transformation using the matrix (4.2). This summarizes the general procedure for finding of the GF $\hat{G}_n(r, r') = \hat{G}_n^{(N)}(r, r')$.

As an application of the general setup, Section 5 considers a cylindrical waveguide with dielectric function $\varepsilon_0(\omega)$ surrounded by a homogeneous medium with permittivity $\varepsilon_1(\omega)$. For convenience of the presentation of formulas, we define the function $\hat{G}^{(c)}(r, r')$ as given in (5.11). For points inside the cylinder, this function describes the effects of the exterior medium (the effects of nonzero difference $\varepsilon_1 - \varepsilon_0$), and for points in the exterior medium, it gives the contribution induced by the cylinder. All the components of the matrix $\hat{G}^{(c)}(r, r')$ are found. The components $G_{2l}^{(c)}(r, r')$, with $l = 1, 2$, become zero. The non-zero components in the interior and exterior regions are given by (5.15), (5.18), (5.20), and (5.23). Knowledge of these components enables investigation of the radiation fields for the general case of a radiating source $\mathbf{j}(r)$. Section 6, discusses general features for three different types of radiation. These correspond to the radiation at large distances from the cylinder, radiation in the form of guided modes of the cylinder, and radiation in the form of surface polaritons localized near the cylinder surface. The latter type of radiation is present in the spectral range where the dielectric permittivities of the neighboring media have opposite signs. Conditions for the appearance of strong peaks in the angular distribution of the radiation propagating at large distances from the cylinder are specified. An equation is derived for the location of these peaks.

In the second part of the paper, a point charge q that rotates around a cylinder with constant velocity v is considered as a radiation source. In Section 8, the expressions for the scalar and vector potentials, and for the electric and magnetic fields inside and outside the cylinder are presented. These fields are used to investigate the spectral-angular density of the radiation intensity. For a given harmonic n , the angular density of the radiation intensity at large distances from the cylinder is expressed as (8.7), with the functions $W_n^{(p)}$ defined in (8.5). Analyzing the presence of narrow peaks in the particular case of the radiation source under consideration confirms the conditions specified for the general case. The necessary conditions $\varepsilon_0 > \varepsilon_1$ and $v_c\sqrt{\varepsilon_0} > c$ are required for those peaks, where v_c is the projection of the particle velocity onto the cylinder surface. Under these conditions, the peaks are located in the angular region (8.11). A numerical analysis of the radiation intensity shows that the results of the general analytic estimates of the peak positions coincide with the data obtained by numerical calculations with high accuracy.

Section 9 studies the electromagnetic fields and energy fluxes of radiation from a circulating charge in the form of the waveguide normal modes. These parts of the total field originate from the poles of the GF, which are the zeros of the function $\alpha_n(k)$. The rules for specifying the integration contour near these poles are dictated by introducing a small imaginary part to the dielectric permittivity. The radiation fields have the structure (9.3), where the radial functions for the magnetic and electric fields are given by the expressions (9.10), (9.11) inside the cylinder and by (9.12), (9.13) in the region $r > r_1$. As an energetic characteristic of the radiated waves, the energy flux through a plane perpendicular to the cylinder's axis is considered. For guided modes, the fluxes in the interior and exterior regions are given by the expressions (9.19) and (9.20), respectively. A simpler expression (9.23) is obtained for the total energy flux by combining the fluxes inside and outside the cylinder. The radiated power, being the work done by the radiation field on the charge per unit time, has been shown to be equal to twice the total energy flux in the region $z > 0$. The features of distribution of the radiated surface polaritonic modes and the corresponding energy fluxes in the exterior and interior regions are discussed in Section 10. The fluxes are positive/negative in a medium with positive/negative permittivity. The total energy flux and

the radiated power are also studied. It has been demonstrated that the number of quanta radiated in the form of surface polaritons can be significantly greater than the corresponding quantity for guided modes.

Acknowledgments

A.A.S. was supported by the grant No. 21AG-1C047 of the Higher Education and Science Committee of the Ministry of Education, Science, Culture and Sport RA. L.Sh.G. and H.F.Kh. were supported by the grant No. 21AG-1C069 of the Higher Education and Science Committee of the Ministry of Education, Science, Culture and Sport RA.

References

- [1] Jelly, J.V., 1958. Cerenkov Radiation and Its Applications, Pergamon, London.
- [2] Zrelov, V.P., 1970. Vavilov-Cherenkov Radiation in High-Energy Physics. Israel Program for Scientific Translations, Jerusalem.
- [3] Afanasieff, G.N., 2004. Vavilov-Cherenkov and Synchrotron Radiation, Springer, Netherlands.
- [4] Ter-Mikaelian, M.L., 1972. High Energy Electromagnetic Processes in Condensed Media, Wiley Interscience, New York.
- [5] Gharibian, G.M., Yan, S., 1983. Rentgenovskoye Perekhodnoye Izluchenie, Izd. AN Arm. SSR, Yerevan in Russian.
- [6] Ginzburg, V.L., Tsytovich, V.N., 1990. Transition Radiation and Transition Scattering, Adam Hilger, Bristol.
- [7] Rullhusen, P., Artru, X., Dhez, P., 1998. Novel Radiation Sources Using Relativistic Electrons. World Scientific, Singapore.
- [8] Potylitsyn, A.P., Ryazanov, M.I., Strikhanov, M.N., Tishchenko, A.A., 2011. Diffraction Radiation from Relativistic Particles, Springer, Netherlands.
- [9] Doucas, G., 2015. Smith-Purcell Radiation: Basic Theory and Applications, Oxford University Press, Oxford.
- [10] Marqués, R., Martín, F., Sorolla, M., 2008. Metamaterials with Negative Parameters: Theory, Design, and Microwave Applications, John Wiley & Sons, Hoboken, NJ.
- [11] Tong, X.C., 2018. Functional Metamaterials and Metadevices, Springer, Netherlands..
- [12] Yeh, C., Shimabukuro, F., 2008. The Essence of Dielectric Waveguides, Springer, Netherlands.
- [13] Atakaramians, S., Afshar, V.S., Monro, T.M., Abbott, D., 2013. Terahertz dielectric waveguides. *Adv. Opt. Photonics* 5, 169.
- [14] Bolotovskii, B.M., 1962. Theory of the vavilov-cherenkov effect (III). *Phys. Usp.* 4, 781.
- [15] Chu, Y.T. et. al., 1984. Contribution of the surface plasmon to energy losses by electrons in a cylindrical channel. *Particle Accelerators* 16, 13.
- [16] De Zutter, D., De Vleeschauwer, D., 1986. Radiation from and force acting on a point charge moving through a cylindrical hole in a conducting medium. *J. Appl. Phys.* 59, 4146.

- [17] Zabala, N., Rivacoba, A., Echenique, P.M., 1989. Energy loss of electrons travelling through cylindrical holes. *Surf. Sci.* 209, 465.
- [18] Walsh, C.A., 1989. Analysis of electron energy-loss spectra from electron-beam-damaged amorphous AlF_3 . *Philos. Mag. A* 59, 227.
- [19] Schmeits, M., 1989. Surface-plasmon coupling in cylindrical pores. *Phys. Rev. B* 39, 7567.
- [20] Grigorian, L.Sh., Saharian, A.A., Iskandarian, A.S., 1990. Green function of classical electromagnetic field in case of coaxial cylindrical layers. *Izv. Nats. Akad. Nauk Arm., Fiz.* 25, 321 (Engl. Transl.: *J. Contemp. Phys.*).
- [21] Walsh, C.A., 1991. An analytical expression for the energy loss of fast electrons traveling parallel to the axis of a cylindrical interface. *Philos. Mag. B* 63, 1063.
- [22] Rivacoba, A., Ape, P., Zabala, N., 1995. Energy loss probability of STEM electrons in cylindrical surfaces. *Nucl. Inst. and Meth. B* 96, 465.
- [23] Grigorian, L.Sh., Kotanjian, A.S., Saharian, A.A., 1995. Electromagnetic field Green function in cylindrically-symmetric inhomogeneous medium. *Izv. Nats. Akad. Nauk Arm., Fiz.* 30, 239 (Engl. Transl.: *J. Contemp. Phys.*).
- [24] Pitarke, J.M., Rivacoba, A., 1997. Electron energy loss for isolated cylinders. *Surf. Sci.* 377, 294.
- [25] Kotanjyan, A.S., Khachatryan, H.F., Petrosyan, A.V., Saharian, A.A., 2000. On features of radiation from charged particle rotating around a dielectric cylinder. *Izv. Nats. Akad. Nauk Arm., Fiz.* 35, 115 (Engl. Transl.: *J. Contemp. Phys.*).
- [26] Arista, N.R., Fuentes, M.A., 2001. Interaction of charged particles with surface plasmons in cylindrical channels in solids. *Phys. Rev. B* 63, 165401.
- [27] Kotanjyan, A.S., Saharian, A.A., 2001. Synchrotron radiation from a charge inside a cylindrical waveguide with dielectric filling. *Izv. Nats. Akad. Nauk Arm., Fiz.* 36, 310 (Engl. Transl.: *J. Contemp. Phys.*).
- [28] Zabala, N., Ogando, E., Rivacoba, A., García de Abajo, F.J., 2001. Inelastic scattering of fast electrons in nanowires: A dielectric formalism approach. *Phys. Rev. B* 64, 205410.
- [29] Kotanjyan, A.S., Saharian, A.A., 2002. Radiation from a charge circulating inside a waveguide with dielectric filling. *Mod. Phys. Lett. A* 17, 1323.
- [30] Wang, Y.-N., Mišković, Z.L., 2002. Energy loss of charged particles moving in cylindrical tubules. *Phys. Rev. A* 66, 042904.
- [31] Kotanjyan, A.S., Saharian, A.A., 2002. Radiation from an electron rotating inside a dielectric cylinder. *Izv. Nats. Akad. Nauk Arm., Fiz.* 37, 263 (Engl. Transl.: *J. Contemp. Phys.*).
- [32] Gervasoni, J.L., Arista, N.R., 2003. Plasmon excitation in cylindrical wires by external charged particles. *Phys. Rev. B* 68, 235302.
- [33] Kotanjyan, A.S., Saharian, A.A., 2003. Radiation from an oscillator inside a cylindrical waveguide with dielectric filling. *Izv. Nats. Akad. Nauk Arm., Fiz.* 38, 288 (Engl. Transl.: *J. Contemp. Phys.*).
- [34] García de Abajo, F.J., Rivacoba, A., Zabala, N., Yamamoto, N., 2004. Boundary effects in Cherenkov radiation. *Phys. Rev. B* 69, 155420.

- [35] Saharian, A.A., Kotanjyan, A.S., 2004. Radiation from an oscillator uniformly moving along the axis of a dielectric cylinder. *Nuclear Instruments and Methods in Physics Research B*, 226, 351 (2004).
- [36] Aligia, A.A., Gervasoni, J.L., Arista, N.R., 2004. Stopping force on point charges in cylindrical wires. *Phys. Rev. B* 70, 235331.
- [37] Grigoryan, L.Sh., Khachatryan, H.F., Saharian, A.A., Kotanjyan, Kh.V., Arzumanyan, S.R., Grigoryan, M.L., 2005. A high power quasi-Cherenkov radiation from a chain of charges in waveguide. *Izv. Nats. Akad. Nauk Arm., Fiz.* 40, 155 (Engl. Transl.: *J. Contemp. Phys.*).
- [38] Saharian, A.A., Kotanjyan, A.S., 2005. Synchrotron radiation from a charge moving along a helical orbit inside a dielectric cylinder. *J. Phys. A* 38, 4275.
- [39] Segui, S., Gervasoni, J.L., Arista, N.R., 2007. Plasmon excitation in nanotubes. Comparison with capillaries and wires. *Radiat. Phys. Chem.* 76, 582.
- [40] Arzumanyan, S.R., Grigoryan, L.Sh., Khachatryan, H.F., Kotanjyan, A.S., Saharian, A.A., 2008. On features of the radiation from an electron moving along a helix inside a cylindrical hole in a homogeneous dielectric. *Nucl. Instr. Methods B* 266, 3703.
- [41] Kotanjyan, A.S., Saharian, A.A., 2007. Electromagnetic field and radiation for a charge moving along a helical trajectory inside a waveguide with dielectric filling. *J. Phys. A: Math. Theor.*, 40 10641.
- [42] Saharian, A.A., Kotanjyan, A.S., Grigoryan, M.L., 2007. Electromagnetic field generated by a charge moving along a helical orbit inside a dielectric cylinder. *J. Phys. A* 40, 1405.
- [43] Aizpurua, J., Rivacoba, A., 2008. Nonlocal effects in the plasmons of nanowires and nanocavities excited by fast electron beams. *Phys. Rev. B* 78, 035404.
- [44] Saharian, A.A., Kotanjyan, A.S., 2009. Synchrotron radiation from a charge moving along a helix around a dielectric cylinder. *J. Phys. A* 42, 135402.
- [45] García de Abajo, F.J., 2010. Optical excitations in electron microscopy. *Rev. Mod. Phys.* 82, 209.
- [46] Hyun, J.K., Levendorf, M.P., Blood-Forsythe, M., Park, J., Muller, D.A., 2010. Relativistic electron energy loss spectroscopy of solid and core-shell nanowires. *Phys. Rev. B* 81, 165403.
- [47] Andonian, G. et al., 2011. Resonant excitation of coherent Cerenkov radiation in dielectric lined waveguides. *Appl. Phys. Lett.* 98, 202901.
- [48] Saharian, A.A., Kotanjyan, A.S., 2012. Synchrotron radiation inside a dielectric cylinder. *Int. J. Mod. Phys. B* 26, 1250033.
- [49] Kotanjyan, A.S., Saharian, A.A., 2013. Undulator radiation inside a dielectric waveguide. *Nucl. Instr. Methods B* 309, 177.
- [50] Yalunin, S.V., Schroder, B., Ropers, C. 2016. Theory of electron energy loss near plasmonic wires, nanorods, and cones. *Phys. Rev. B* 93, 115408.
- [51] Kotanjyan, A.S., Mkrtchyan, A.R., Saharian, A.A., Kotanjyan, V.Kh., 2018. Radiation of surface waves from a charge rotating around a dielectric cylinder, *JINST* 13, C01016.
- [52] Galyamin, S.N., Tyukhtin, A.V., Vorobev, V.V., Grigoreva, A.A., Aryshev, A.S., 2019. Cherenkov radiation of a charge exiting open-ended waveguide with dielectric filling. *Phys. Rev. Spec. Top. Accel. Beams* 22, 012801.

[53] Kotanjyan, A.S., Mkrtchyan, A.R., Saharian, A.A., Kotanjyan, V.Kh., 2019. Generation of surface polaritons in dielectric cylindrical waveguides. *Phys. Rev. Spec. Top. Accel. Beams* 22, 040701.

[54] Jiang, S., Li, W., He, Z., Huang, R., Jia, Q., Wang, L., Lu, Y., 2019. High power THz coherent Cherenkov radiation based on a separated dielectric loaded waveguide. *Nucl. Instrum. Meth. A* 92, 45.

[55] Saharian, A.A., Kotanjyan, A.S., Kotanjyan, V.Kh., 2019. Synchrotron radiation from a charge on eigenmodes of a dielectric cylinder. *J. Contemp. Phys.* 54, 111.

[56] Mkrtchyan, A.R., Grigoryan, L.S., Saharian, A.A., Mkrtchyan, A.H., Khachatryan, H.F., Kotanjyan, V.K., 2020. Self-amplification of radiation from an electron bunch inside a waveguide filled with periodic medium. *JINST* 15, C06019.

[57] Saharian, A.A., Grigoryan, L.Sh., Grigorian, A.Kh., Khachatryan, H.F., Kotanjyan, A.S., 2020. Cherenkov radiation and emission of surface polaritons from charges moving paraxially outside a dielectric cylindrical waveguide. *Phys. Rev. A* 102, 063517.

[58] Saharian, A.A., Kotanjyan, A.S., Grigoryan, L.Sh., Khachatryan, H.F., Kotanjyan, V.Kh., 2020. Synchrotron radiation from a charge circulating around a cylinder with negative permittivity. *Int. J. Mod. Phys. B* 34, 2050065.

[59] Saharian, A.A., Grigoryan, L.Sh., Kotanjyan, A.S., Khachatryan, H.F., 2023. Surface polariton excitation and energy losses by a charged particle in cylindrical waveguides. *Phys. Rev. A* 107, 063513.

[60] Saharian, A.A., Dabagov, S.B., Khachatryan, H.F., Grigoryan, L.Sh., 2024. Quasidiscrete spectrum Cherenkov radiation by a charge moving inside a dielectric waveguide. *JINST* 19, C06017.

[61] Saharian, A.A., Chalyan, G.V., Grigoryan, L.Sh., Khachatryan, H.F., Kotanjyan, V.Kh., 2025. Radiation of surface polaritons by an annular beam coaxially enclosing a cylindrical waveguide. *Nucl. Instr. Methods B* 1075, 170408.

[62] Kitao, K., 1960. Energy loss and radiation of a gyrating charged particle in a magnetic field. *Prog. Theor. Phys.* 23, 759.

[63] Erber, T., White, D., Latal, H.G., 1976. Inner bremsstrahlung processes. I. *Acta Phys. Austriaca* 45, 29.

[64] Schwinger, J., Tsai, W.-Y., Erber, T., 1976. Classical and quantum theory of synergic synchrotron-Čerenkov radiation. *Ann. Phys.* 96, 303.

[65] Erber, T., White, D., Tsai, W.-Y., Latal, H.G., 1976. Experimental aspects of synchrotron-Čerenkov radiation. *Ann. Phys.* 102, 405.

[66] Rynne, T.M., Baumgartner, G.B., Erber, T., 1978. The angular distribution of synchrotron-Čerenkov radiation. *J. Appl. Phys.* 49, 2233.

[67] Bonin, K.D., McDonald, K.T., Russell, D.P., Flanz, J.B., 1986. Observation of interference between Čerenkov and synchrotron radiation. *Phys. Rev. Lett.* 57, 2264.

[68] García de Abajo, F.J., Howie, A., 2002. Retarded field calculation of electron energy loss in inhomogeneous dielectrics. *Phys. Rev. B* 65, 115418.

[69] Galyamin, S.N., Tyukhtin, A.V., 2014. Electromagnetic field in dielectric concentrator for Cherenkov radiation. *Phys. Rev. Lett.* 113, 064802.

[70] Belonogaya, E.S., Galyamin, S.N., Tyukhtin, A.V., 2015. Short-wavelength radiation of a charge moving in the presence of a dielectric prism. *J. Opt. Soc. Am. B* 32, 649.

[71] Kotanjyan, A.S., Mkrtchyan, A.R., Saharian, A.A., 2017, Radiation from a charge rotating inside a cylindrical grating. *Nucl. Instr. Methods B* 402, 173.

[72] Saharian, A.A., Kotanjyan, A.S., Mkrtchyan, A.R., Khachatryan, B.V., 2017. Synchrotron and Smith-Purcell radiations from a charge rotating around a cylindrical grating. *Nucl. Instr. Methods B* 402, 162.

[73] Tyukhtin, A., Vorobev, V., Belonogaya, E., Galyamin, S., 2018. Cherenkov radiation of a charge flying through the "inverted" conical target. *JINST* 13, C02033.

[74] Tyukhtin, A.V., Galyamin, S.N., Vorobev, V.V., 2019. Peculiarities of Cherenkov radiation from a charge moving through a dielectric cone. *Phys. Rev. A* 99, 023810.

[75] Grigoryan, L.Sh., et al., 2024. Observation of coherent Cherenkov radiation of electron bunches from a partially dielectric loaded waveguide. *Nucl. Instr. Methods A* 1062, 169177.

[76] Grigoryan, L.Sh., et al., 2026. Observation of coherent Cherenkov diffraction radiation modes in a long cylindrical Teflon radiator. *Rad. Phys. Chem.* 240, 113435.

[77] Jackson, J.D., 1999. *Classical Electrodynamics*, John Wiley and Sons, Inc.

[78] Maier, S.A., 2007. *Plasmonics: Fundamentals and Applications*. Springer, New York.

[79] Enoch, S., Bonod, N. (Editors), 2012. *Plasmonics: From Basics to Advanced Topics*. Springer, New York.

[80] Stockman, M.I., et al., 2018. Roadmap on plasmonics, *J. Optics* 20, 043001.

[81] Ashley, J.C., Emerson, L.C., 1974. Dispersion relations for non-radiative surface plasmons on cylinders. *Surf. Sci.* 41, 615.

[82] Khosravi, H., Tilley, D.R., Loudon, R., 1991. Surface polaritons in cylindrical optical fibers. *J. Opt. Soc. Am. A* 8, 112.

[83] Abramowitz, M., Stegun, I.A. (Editors), 1972. *Handbook of Mathematical Functions*. New York, Dover.

[84] Prudnikov, A.P., Brychkov, Yu.A., Marichev, O.I., 1990. *Integrals and Series*. Gordon and Breach, New York, Vol. 2.

[85] Han, Zh., Bozhevolnyi, S.I., 2013. Radiation guiding with surface plasmon polaritons, *Rep. Prog. Phys.* 76, 016402.

[86] Gong, S., Hu, M., Zhong, R., Chen, X., Zhang, P., Zhao, T., Liu, S., 2014. Electron beam excitation of surface plasmon polaritons. *Optics Express* 22, 19252.